Free Radical Biology and Medicine 208 (2023) 478–493

Contents lists available at ScienceDirect

Free Radical Biology and Medicine

journal homepage: www.elsevier.com/locate/freeradbiomed

Nrf2 depletion in the context of loss-of-function Keap1 leads to mitolysosome accumulation

Sharadha Dayalan Naidu [a,1], Plamena R. Angelova [b,1], Elena V. Knatko [a], Chiara Leonardi [a], Miroslav Novak [a], Laureano de la Vega [a], Ian G. Ganley [c], Andrey Y. Abramov [b,**], Albena T. Dinkova-Kostova [a,d,*]

[a] Jacqui Wood Cancer Centre, Division of Cellular and Systems Medicine, School of Medicine, University of Dundee, Dundee, UK
[b] UCL Queen Square Institute of Neurology, Queen Square, London, UK
[c] MRC Protein Phosphorylation and Ubiquitylation Unit, School of Life Sciences, University of Dundee, Dundee, UK
[d] Department of Pharmacology and Molecular Sciences and Department of Medicine, Johns Hopkins University School of Medicine, Baltimore, MD, USA

A B S T R A C T

Transcription factor nuclear factor erythroid 2 p45-related factor 2 (Nrf2) is the principal determinant of the cellular redox homeostasis, contributing to mitochondrial function, integrity and bioenergetics. The main negative regulator of Nrf2 is Kelch-like ECH associated protein 1 (Keap1), a substrate adaptor for Cul3/Rbx1 ubiquitin ligase, which continuously targets Nrf2 for ubiquitination and proteasomal degradation. Loss-of-function mutations in Keap1 occur frequently in lung cancer, leading to constitutive Nrf2 activation. We used the human lung cancer cell line A549 and its CRISPR/Cas9-generated homozygous Nrf2-knockout (Nrf2-KO) counterpart to assess the role of Nrf2 on mitochondrial health. To confirm that the observed effects of Nrf2 deficiency are not due to clonal selection or long-term adaptation to the absence of Nrf2, we also depleted Nrf2 by siRNA (si*NFE2L2*), thus creating populations of Nrf2-knockdown (Nrf2-KD) A549 cells. Nrf2 deficiency decreased mitochondrial respiration, but increased the mitochondrial membrane potential, mass, DNA content, and the number of mitolysosomes. The proportion of ATG7 and ATG3 within their respective LC3B conjugates was increased in Nrf2-deficient cells with mutant Keap1, whereas the formation of new autophagosomes was not affected. Thus, in lung cancer cells with loss-of-function Keap1, Nrf2 facilitates mitolysosome degradation thereby ensuring timely clearance of damaged mitochondria.

1. Introduction

Transcription factor nuclear factor erythroid 2 p45-related factor 2 (Nrf2, gene name *NFE2L2*) and its main negative regulator Kelch-like ECH associated protein 1 (Keap1) control the coordinate expression of a battery of genes encoding proteins, which allow adaptation and survival under conditions of stress [1,2]. At homeostatic conditions, Keap1 serves as a substrate adaptor for Cul3/Rbx1-based ubiquitin ligase that continuously targets Nrf2 for ubiquitination and proteasomal degradation [3–5]. Electrophiles and oxidants (termed inducers) react with specific cysteine sensors of Keap1 [6], inhibiting its substrate adaptor function, and resulting in Nrf2 accumulation and transcriptional activation of its target genes encoding proteins with diverse cytoprotective functions. The critical importance of the Keap1/Nrf2 system in human health is highlighted by the fact that it is frequently dysregulated (either down- or upregulated) in disease, and is now considered a drug target [7]. A number of small molecule pharmacological activators are currently in various stages of clinical development for several disease indications [8,9], and two compounds, dimethyl fumarate (Tecfidera™) and omaveloxolone (RTA-408; Skyclarys™) are in clinical practice for the treatment of relapsing-remitting multiple sclerosis and Friedreich's ataxia, respectively [7,10].

The Nrf2-regulated genes encode proteins that take part in xenobiotic detoxification, regulate redox and protein homeostasis, and promote repair processes. Nrf2 also affects intermediary metabolism, mitochondrial function and bioenergetics [11], in part through promoting fatty acid oxidation [12], and its upregulation has features of fasted metabolic state [13]. In addition, Nrf2 regulates the expression of genes that function in autophagy, including the gene encoding the critical autophagy cargo protein p62/Sequestosome 1 (SQSTM1) [14,

* Corresponding author. Jacqui Wood Cancer Centre, Division of Cellular Medicine, Ninewells Hospital and Medical School, James Arrott Drive, Dundee, DD1 9SY, UK.
** Corresponding author. UCL Queen Square Institute of Neurology, Queen Square, London, WC1N 3BG, UK.
E-mail addresses: a.abramov@ucl.ac.uk (A.Y. Abramov), a.dinkovakostova@dundee.ac.uk (A.T. Dinkova-Kostova).
[1] Co-first authors.

https://doi.org/10.1016/j.freeradbiomed.2023.09.009
Received 8 August 2023; Received in revised form 8 September 2023; Accepted 10 September 2023
Available online 14 September 2023

15], as well as multiple genes involved in both macroautophagy as well as chaperone-mediated autophagy [16,17]. This is consistent with findings that genetic (by inactivation of Keap1) or pharmacologic Nrf2 activation promotes, whereas Nrf2 depletion impairs autophagic flux [13,18,19]. However, the molecular details are incompletely understood.

In addition to their effects on autophagy, Keap1 and Nrf2 have been implicated in mitophagy. It has been shown that, in parallel to the PINK1-Parkin pathway of mitophagy, p62 recruits Keap1 and Rbx1 to mitochondria to promote ubiquitination that labels damaged mitochondria for mitophagy [20,21]. A non-electrophilic Nrf2 activator called p62-mediated mitophagy inducer (PMI), which disrupts the protein-protein interactions between Keap1 and Nrf2 [22], induces mitophagy without dissipating the mitochondrial membrane potential or Parkin recruitment [23]. PMI induces mitochondrial respiration and the expression of p62 [24]. Similarly to PMI, other Keap1-Nrf2 protein-protein interaction inhibitors also induce mitophagy [24]. However the electrophilic Nrf2 inducers sulforaphane and dimethyl fumarate, which covalently modify cysteines in Keap1, are unable to induce such response [24], even though Nrf2 regulates the expression of several autophagy-related genes [16,17], and its activation by sulforaphane and other electrophilic inducers promotes autophagy [18,19]. In fact, co-treatment of PMI with sulforaphane was shown to inhibit some of the PMI-induced effects required for mitophagy [24]. Yet, both electrophilic and non-electrophilic Nrf2 activators induce similar alterations on mitochondrial morphology and bioenergetic profiles, suggesting that the reversible inhibition of the Keap1-Nrf2 protein-protein interactions by PMI is important for activation of mitophagy [24]. In addition, the PINK1-Parkin pathway was not required for mitophagy induced by PMI, but Nrf2 was [23–25].

During autophagosome formation, LC3 undergoes lipidation, whereby LC3 is conjugated to phosphatidylethanolamine (PE), first through the formation of an amide bond between the *C*-terminal glycine of the E1-like conjugating enzyme AuTophaGy regulator 7 (ATG7) and the amino group of PE, followed by transfer to the E2-like conjugating enzyme ATG3 [26]. Frudd et al. have described that under conditions of oxidative stress, the amino acid starvation-mediated LC3 lipidation is inhibited, due to cysteine oxidation within ATG3 and ATG7 [27]. Nrf2 is the principal determinant of the cellular redox homeostasis by regulating the expression of thioredoxin, thioredoxin reductase, and the enzymes that catalyze the biosynthesis and regeneration of reduced glutathione (GSH) and NADPH [2]. This is particularly important in the context of loss-of-function mutations in Keap1, a common occurrence in lung cancer [28], where the resultant constitutive activation of Nrf2 counteracts oncogene-driven increased generation of reactive oxygen species [29]. We therefore hypothesized that Nrf2 activity may affect mitophagy through control of redox balance. To test this hypothesis, we used the human lung cancer cell line A549 and its CRISPR/Cas9-generated homozygous Nrf2-knockout (Nrf2-KO) counterpart [30]. The A549 cell line has constitutively high Nrf2 levels due to a combination of lower expression of Keap1 and a homozygous mutation (G333C) in the Kelch domain of Keap1, the site of interaction between Keap1 and Nrf2 [31]. To confirm that the observed effects of Nrf2 deficiency are not due to clonal selection or long-term adaptation to the absence of Nrf2, for some experiments we also depleted Nrf2 by siRNA (si*NFE2L2*), creating populations of Nrf2-knockdown (Nrf2-KD) A549 cells. Thus, this experimental system (i.e. A549 Nrf2-KO or Nrf2-KD, and A549 Nrf2-WT cells) represents two extreme conditions, namely Nrf2 deficiency vs. Nrf2 constitutive activation. We found that Nrf2 deficiency decreased mitochondrial respiration and cellular ATP levels, but surprisingly, increased the mitochondrial membrane potential, mass, DNA content, and the number of mitolysosomes per cell. Moreover, Nrf2 deficiency increased the proportion of ATG7 and ATG3 within their respective LC3B conjugates without affecting the formation of new autophagosomes.

2. Results

2.1. Nrf2 deficiency in A549 cells decreases respiration, but increases the mitochondrial membrane potential and reverses the activity of complex V

Compared to wild-type, mitochondrial respiration is decreased in Nrf2-KO mouse embryonic fibroblasts, bone-marrow derived macrophages and primary glio-neuronal cultures isolated from Nrf2-KO mice, whereas respiration is increased in their corresponding Keap1-knockout (Keap1-KO) and Keap1-knockdown (Keap1-KD) counterparts [11,12,32]. In close agreement with these observations, the mitochondrial respiration and the cellular ATP levels were lower in Nrf2-KO in comparison with Nrf2-WT A549 cells (Fig. 1A). The siRNA-mediated knockdown of Nrf2 (Nrf2-KD) had a similar effect to the CRISPR/Cas9-generated Nrf2-KO (Fig. 1B), implying that the observed effects of Nrf2 deficiency were not due to clonal selection or long-term adaptation to the absence of Nrf2.

Next, we measured the mitochondrial membrane potential ($\Delta\Psi_m$), a major indicator of mitochondrial health, using live cell imaging and the cationic fluorescent indicator tetramethylrhodamine methyl ester (TMRM). Nrf2 deficiency induced a 2-fold increase in $\Delta\Psi_m$, depicted as a rise in TMRM intensity, from 976 ± 256 (n = 97) in A549 Nrf2-WT cells to 2196 ± 540 (n = 83) in A549 Nrf2-KO cells; $p < 0.0001$; Fig. 1C). Mitochondria maintain the $\Delta\Psi_m$ mainly by pumping protons out of their matrix through complexes I, III and IV of the electron transport chain (ETC). However, a deficiency in the activity of the ETC in the maintenance of $\Delta\Psi_m$ can be compensated by various mechanisms, including switching the F_oF_1-ATPsynthase to an ATPase mode of Complex V. The inhibitor of the F_oF_1-ATP complex oligomycin inhibits both the ATP synthase and the ATPase activities of this enzyme. Application of 2 μg/ml oligomycin induced a small (about 3–5%) increase of $\Delta\Psi_m$ of A549 Nrf2-WT cells, suggesting that complex V in these cells is working in ATP synthase mode (Fig. 1D; n = 27). Subsequent application of the complex I inhibitor rotenone (5 μM) induced a profound decrease (63 ± 9%, n = 27) in TMRM fluorescence. Application of the uncoupler FCCP (1 μM) at the end of the experiment induced complete mitochondrial depolarization. Considering that after inhibition of F_oF_1-ATPsynthase and complex I, complex II can be the main contributor for delivery of electrons to the ETC, these results indicate a substantial contribution of complex II to the maintenance of $\Delta\Psi_m$ in A549 cells.

Nrf2 deficiency in A549 cells completely changed the effect of oligomycin on the TMRM signal and induced mitochondrial depolarization (by 32 ± 7%; Fig. 1E; n = 33), strongly suggesting that complex V is working in reverse, as ATPase, pumping protons out. Importantly, rotenone induced almost complete depolarization in these cells, and FCCP induced only a minor (5 ± 3%, n = 33) decrease in TMRM fluorescence, which suggests lower activity of complex II in Nrf2-KO compared to Nrf2-WT A549 cells. Thus, A549 cells maintain $\Delta\Psi_m$ by ETC with contributions from complex I and II. Deficiency in Nrf2 switched on a compensatory mechanism, transposing the complex V activity from F_oF_1-ATP synthase to ATPase mode that led to an increased $\Delta\Psi_m$.

2.2. Nrf2 deficiency in A549 cells leads to alterations in the mitochondrial redox state

The lower complex II activity in A549 Nrf2-KO cells led us to assess the mitochondrial redox state. The Nrf2 deficiency did not significantly change the complex I-dependent redox index (Fig. 2A,B,E), but significantly decreased the FAD redox index from 84.3 ± 5.2, n = 24 to 35.6 ± 6.5, n = 21 ($p < 0.0001$) (Fig. 2C–E), which reflects a decrease in complex II activity. The FADH pool, i.e. the difference in responses to NaCN (maximal $FADH_2$ but minimal FAD) and FCCP (minimal FAD but maximal $FADH_2$ in mitochondrial complex II), of A549 Nrf2-KO cells was decreased (from 1000 ± 68, n = 24 to 550 ± 35, n = 21, $p < 0.0001$) in comparison with Nrf2-WT cells (Fig. 2F). The lower FADH

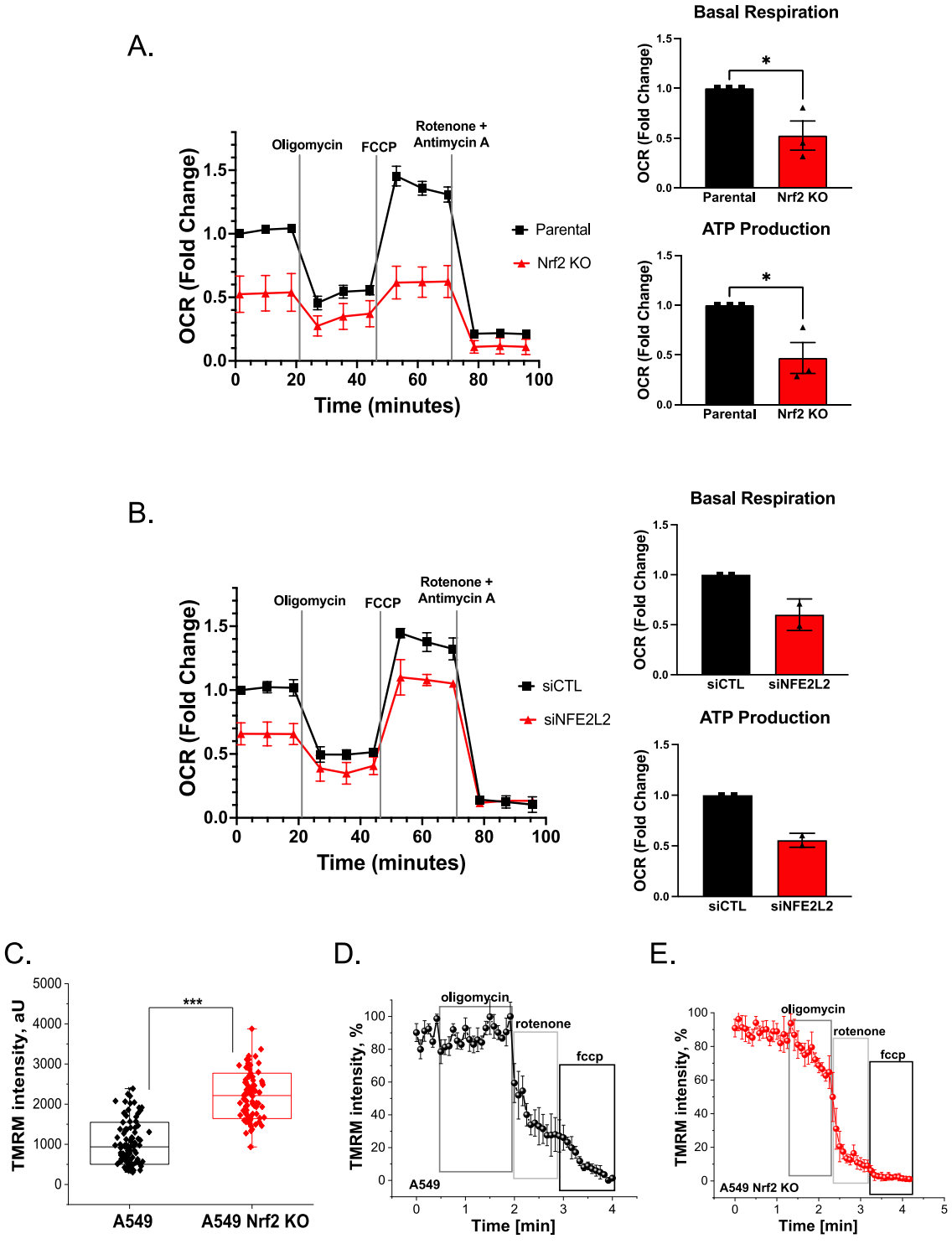

Fig. 1. Nrf2 deficiency in A549 cells decreases respiration and ATP production, but increases the mitochondrial membrane potential and reverses the activity of complex V.

Comparison of real-time oxygen consumption rates (OCR) of cultured A549 cells with their Nrf2-knockout (Nrf2-KO) **(A)** and Nrf2-knockdown (si*NFE2L2*) **(B)** counterparts using the Seahorse XFe24 analyzer where Oligomycin (1 μM), FCCP (1 μM) and Rotenone/Antimycin A (1 μM) were added at the indicated times. The bar graphs show the mean basal respiration and ATP production. Data represented are the means ± SEM of three **(A)** or two **(B)** independent experiments. *$p < 0.05$. **(C)** Mitochondrial membrane potential in A549 and A549 Nrf2-KO cells. **(D,E)** Inhibitor analysis of the mitochondrial membrane potential maintenance and electron transport chain (ETC) function in A549 **(D)** and A549 Nrf2-KO **(E)** cells. Data are presented as mean ± SEM. ***$p < 0.0001$.

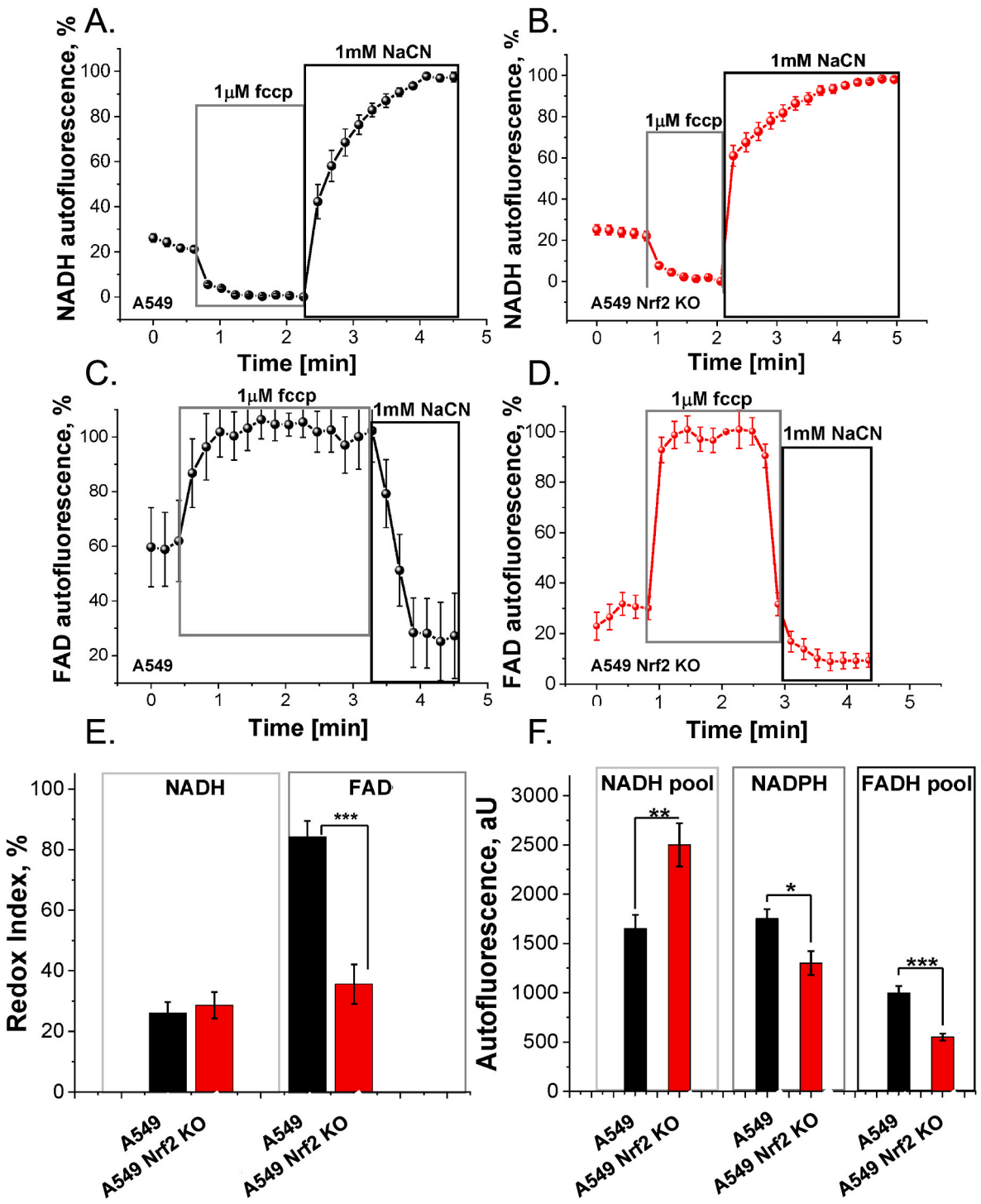

Fig. 2. Nrf2 deficiency in A549 cells leads to a decrease in complex II activity. **(A,B)** Representative traces of mitochondrial respiration through Complex I from A549 (black) **(A)** and A549 Nrf2 KO (red) **(B)** cells as assessed by NADH fluorescence. Representative traces of mitochondrial respiration through complex II from A549 (black) **(C)** and A549 Nrf2-KO (red) **(D)** cells as assessed by FAD fluorescence. Application of 1 μM FCCP maximizes respiration and addition of 1 mM NaCN fully inhibits mitochondrial respiration. **(E)** Quantification of the redox indices of NADH and FADH for A549 (black) and A549 Nrf2-KO (red) cells. **(F)** Quantification bar charts representing changes in the NADH and FADH pools, as well as the NADPH levels in A549 (black) and A549 Nrf2-KO (red) cells. Data are presented as mean ± SEM. *$p < 0.05$, **$p < 0.001$, ***$p < 0.0001$.

pool suggests lower substrates (donor electron availability) for complex II, which could be one reason for the lower activity of this complex. In contrast, compared to Nrf2-WT, the NADH pool was significantly increased in Nrf2-KO cells (from 1650 ± 138, n = 24 to 2500 ± 220, n = 21, p = 0.0084), but the levels of NADPH were lower (Fig. 2F).

2.3. Nrf2 deficiency in A549 cells leads to an increase in mitochondrial ROS production, a decrease in GSH levels and an increase in mitochondrial content

Compensation for the lack of respiratory activity for the maintenance of $\Delta\Psi_m$ by F_oF_1-ATPase activity often leads to an increase in $\Delta\Psi_m$ [33,

34]. Considering that the production of reactive oxygen species (ROS) in mitochondria is dependent on $\Delta\Psi_m$ [35,36], an increase of $\Delta\Psi_m$ would lead to overproduction of ROS in the ETC [33,34,37]. In agreement with the higher $\Delta\Psi_m$ in A549 Nrf2-KO cells, the rate of ROS production by their mitochondria was 2-fold higher than in A549 Nrf2-WT cells (from 40.4 ± 13.2, n = 11 to 76.7 ± 9.8, n = 9, p = 0.0105; Fig. 3A–C). This ROS overproduction in Nrf2-deficient cells was accompanied by a decrease in the level of reduced glutathione (GSH), as shown by the drop of fluorescence when using the monochlorobimane (MCB) probe in these cells, from 2228.8 ± 118.7, n = 53 to 1483.0 ± 55.1, n = 52, compared to Nrf2-WT A549 cells (p < 0.0001; Fig. 3D). In addition to this single-cell analysis, the higher levels of ROS and the corresponding lower levels of GSH in Nrf2-deficient cells were also confirmed in cell populations (Fig. 3E and F).

2.4. Nrf2 deficiency increases the levels of mitochondrial DNA and mitochondrial mass

The level of DNA was estimated using the fluorescent indicator PicoGreen. The level of nuclear PicoGreen-DNA fluorescence was similar between the genotypes (not shown). In contrast to the nuclear signal, the PicoGreen-DNA fluorescence from the mitochondrial area was significantly higher in Nrf2-KO than in Nrf2-WT A549 cells (from 823.1 ± 27.0, n = 30 to 1198.5 ± 51.1, n = 24, p < 0.0001; Fig. 3G), suggesting an increase in mitochondrial content in Nrf2-deficient cells. To explore this possibility further, we measured the fluorescence of the TMRM or/and MitoTracker Green signals. In agreement with the Pico-Green results, the mitochondrial mass in Nrf2-deficient cells was significantly increased in comparison with their Nrf2-WT counterparts (from 1.583 ± 0.094, n = 20 to 7.199 ± 0.638, n = 21, p < 0.0001; Fig. 3H).

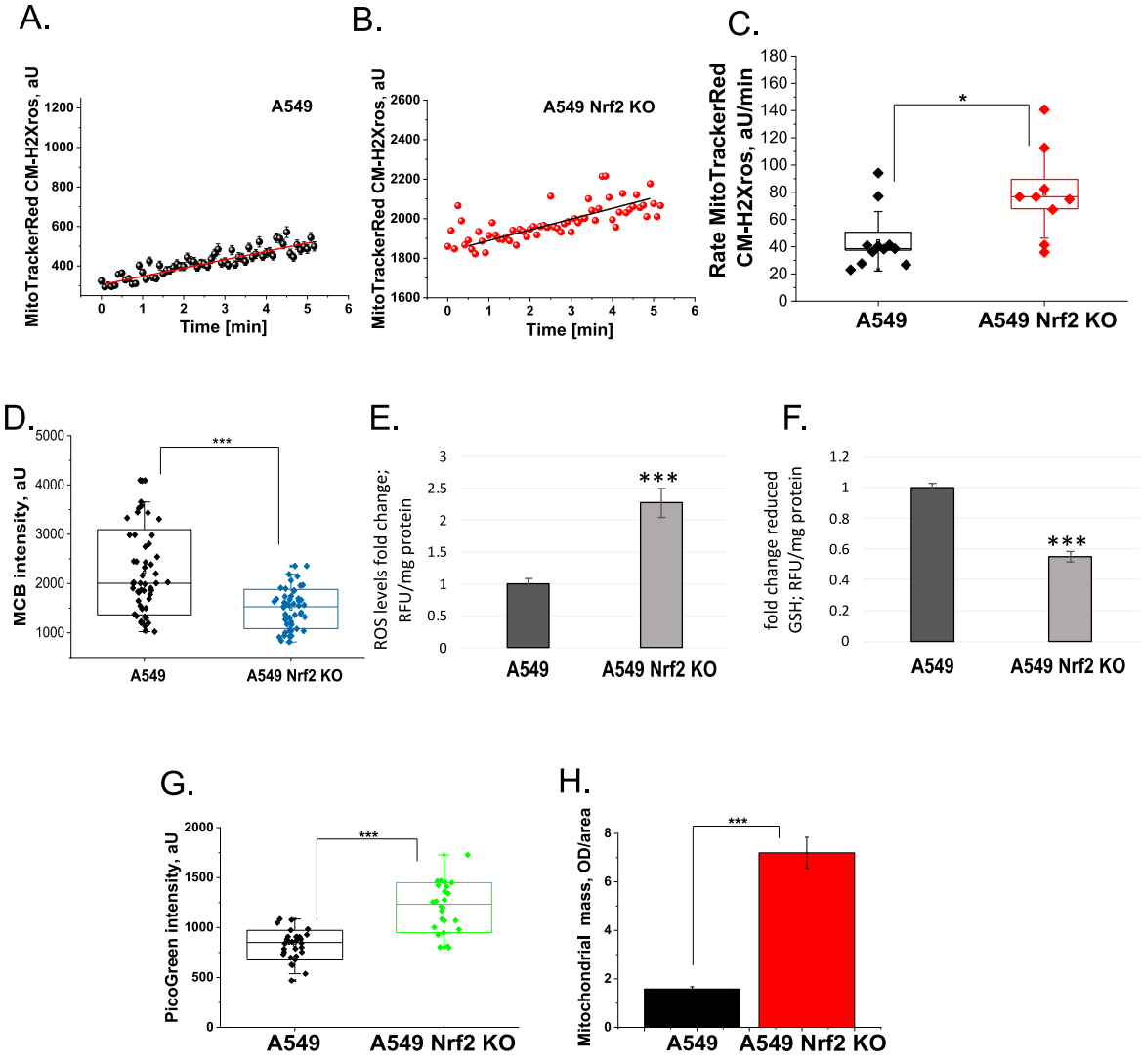

Fig. 3. Nrf2 deficiency in A549 cells leads to an increase in mitochondrial ROS production, a decrease in GSH levels and an increase in mitochondrial content. **(A,B)** Representative traces of the rate of mitochondrial ROS production in A549 **(A)** and A549 Nrf2 KO **(B)** cells as assessed by MitoTracker Red CM-H2XRos. **(C)** Quantification of the ROS production rates for A549 and A549 Nrf2-KO cells. **(D)** Quantification of the levels of GSH in A549 and A549 Nrf2-KO cells as assessed using the monochlorobimane (MCB) probe. **(E,F)** Levels of ROS **(E)** and GSH **(F)** in A549 cells after incubation with 10 μM of H_2DCFDA in HBSS. The levels of ROS were determined by measuring the fluorescence emitted by live cells, using a fluorometer (Ex485/Em538). The levels of GSH were determined following incubation with 120 μM of MCB in HBSS, and the resulting fluorescence was measured using a fluorometer (Ex390nm/Em490). **(G,H)** Quantification of the mtDNA content **(G)** and the mitochondrial mass **(H)** in A549 and A549 Nrf2-KO cells. Data are presented as mean ± SEM. *p < 0.05, ***p < 0.0001.

2.5. Nrf2 deficiency increases the co-localization of mitochondria with lysosomes in A549 cells

The increase in mitochondrial mass and DNA in the Nrf2-KO cells was unexpected, because Nrf2 had been implicated in mitochondrial biogenesis [38]. This led us to consider the possibility that Nrf2 may affect mitophagy. To assess this process, we measured the co-localization of mitochondrial signal (MitoTracker Green) and the lysosome signal (LysoTracker Red DND-99), as described [39]. Nrf2 deficiency increased the co-localization of mitochondria with lysosomes, from 0.667 ± 0.011, n = 169 to 0.864 ± 0.007, n = 197 ($p < 0.0001$; Fig. 4A–C). This result was initially surprising, because it suggested that mitophagy was enhanced, whereas the increased mitochondrial membrane potential, mass and DNA content (Figs. 1C and 3G, H), taken together with the decreased respiration (Fig. 1A and B) and the increased ROS production (Fig. 3A–C) and overall ROS levels (Fig. 3E) in Nrf2-KO A549 cells, was indicative that mitophagy was impaired. We then considered the possibility that the number of lysosomes might differ between the genotypes, but their quantification showed that Nrf2-KO A549 cells have less, not more, lysosomes than their Nrf2-WT counterparts (Fig. 4D–G). Of note, the images revealed higher pH in lysosomes of Nrf2-KO A549 cells, which could potentially affect mitolysosomal processing. Thus, the difference in the number of lysosomes did not provide an explanation for the increased number of mitolysosomes in Nrf2-deficient cells.

To further confirm the effect of Nrf2 deficiency on mitolysosome accumulation, we used A549 cells that stably express a tandem mCherry-GFP fluorescent tag fused to the outer mitochondrial membrane localization signal of the mitochondrial protein FIS1 [40]. Under basal conditions, the fluorescence from these cells is red and green. When mitophagy is stimulated and the mitochondria are fused to lysosomes, the acidic environment quenches the GFP signal, but not the mCherry signal, resulting in formation of puncta with only red fluorescence, which represent the mitolysosomes. Using this experimental system, we compared the number of mitolysosomes in cells that had been transfected for 96 h with either control siRNA (siCTL) or si*NFE2L2*, which resulted in a highly efficient knockdown of Nrf2 (Fig. 4H). This assay too, showed that Nrf2 knockdown led to an increase in the number of mitolysosomes per cell (Fig. 4I–K), both basally as well as upon stimulation with the iron chelator deferiprone (DFP, used as a positive control for induction of mitophagy) [40].

2.6. Nrf2 deficiency impairs the lipidation of LC3B

Next, we considered impaired autophagy as an explanation for the increased mitolysosome accumulation in Nrf2-deficient A549 cells. We previously observed that compared to Nrf2-WT, Nrf2-KO A549 cells have lower levels of the lipidated form of LC3B, LC3B-II, and reduced autophagic flux [13]. We confirmed that the levels of the non-lipidated form of LC3B, LCB-I, were higher in Nrf2-KO A549 cells than in the parental Nrf2-WT cell line (Fig. 5A, top LC3B blot), whereas the levels of the lipidated form of LC3B, LC3B-II, were lower (Fig. 5A, bottom LC3B blot). Of note, two different membranes were used for the immunoblotting of LC3B, because LC3B–I is detected better on a nitrocellulose (NC) membrane, whereas the use of polyvinylidene difluoride (PVDF) membrane is more appropriate for detecting LC3B-II [41]. Treatment of Nrf2-KO A549 cells with the cell permeable form of glutathione, glutathione ethyl ester (GSH-EE), increased the levels of GSH (Fig. 5B), and partially rescued LC3B lipidation, implying that the high levels of ROS in the absence of Nrf2 (Fig. 3A–C,E) are involved in inhibition of LC3B lipidation. Interestingly, treatment with buthionine sulfoximine (BSO), an inhibitor of GSH biosynthesis, decreased the levels of GSH in both genotypes (Fig. 5B), and increased the lipidation of LC3B in A549 cells, but not in Nrf2-KO A549 cells. Considering that BSO treatment has been previously shown to enhance LC3 lipidation and activate autophagy in retinal pigment epithelial [42], spermatogonial [43] and A549 [44] cells, this result further confirms that LC3B lipidation is impaired in the absence of Nrf2. Overall, the decreased LC3B lipidation in Nrf2 deficiency suggests that autophagy is impaired.

2.7. Nrf2 deficiency increases the proportion of ATG7 and ATG3 within their respective LC3 conjugates

The redox sensitivity of ATG3 and ATG7 [27], together with the lower levels of GSH (Fig. 3D,F and 5B) and the higher levels of ROS (Fig. 3A–C,E) in Nrf2-KO cells, prompted us to examine ATG3 and ATG7. For this purpose, we employed the PEG-switch assay [45]. This assay uses a polyethylene glycol (PEG)-based alkylating agent for semi-quantitative assessment of protein cysteines that are engaged in bonds, which can be broken by reducing agents. In addition to ATG3 and ATG7, we also included in this analysis the cysteine protease ATG4B that mediates the processing of LC3 leading to exposure of its *C*-terminal glycine, which is essential for the subsequent LC3 conjugation to phosphatidylethanolamine. The use of the PEG-switch assay revealed the presence of slower migrating bands for ATG7 and ATG3 in the Nrf2-KO cells (Fig. 6A and B). This assay detected two slower migrating species of ATG3 (indicated with arrows in Fig. 6B), suggesting that, under our experimental conditions, more than one cysteine within ATG3 were engaged in covalent bonds that are cleavable by the reducing agent; notably, both species were present at higher levels in Nrf2-deficient than in Nrf2-proficient cells. Depleting Nrf2 acutely (by siRNA) in A549 cells had a similar effect to that of the Nrf2 knockout in the CRISPR/Cas9-generated A549 cells (Fig. 6A). In contrast, no slower migrating bands for ATG4B were detectable in either Nrf2-WT, Nrf2-KO or Nrf2-KD A549 cells (Fig. 6C).

Next, we compared the levels of the ATG7-LC3 and ATG3-LC3 conjugates (each of which is formed through a thioester bond) in Nrf2-WT and Nrf2-KO A549 cells using non-reducing sodium dodecyl sulfate polyacrylamide gel electrophoresis (SDS-PAGE). Upon detection of ATG7 and ATG3 (Fig. 6D), we observed higher molecular weight complexes (with a molecular weight approximately 15 kDa greater than that of ATG7 and ATG3, respectively) corresponding to covalently-bound ATG7-LC3 and ATG3-LC3. These complexes were not detectable under reducing conditions, consistent with a thioester bond linkage between ATG7/ATG3 and LC3. Compared to Nrf2-WT, Nrf2-KO A549 cells had a higher proportion of ATG7 and ATG3 within their respective ATG7-LC3 and ATG3-LC3 conjugates: the ratio of LC3 conjugated-to unconjugated ATG7 was increased by ~8.4-fold and the ratio of LC3 conjugated-to unconjugated ATG3 was increased by ~2.6-fold (compare lane 1 with lane 5 in Fig. 6D). These differences between the genotypes were attenuated upon treatment with glutathione ethyl ester (GSH-EE), from ~8.4-fold to ~6.4-fold for ATG7-LC3:ATG7, and from ~2.6-fold to 1.6-fold for ATG3-LC3:ATG3, consistent with redox regulation. Curiously, treatment with bafilomycin A_1 (BAF), which disrupts autophagic flux by inhibiting both the lysosomal proton pump V-ATPase and autophagosome-lysosome fusion [46], led to a decrease in the conjugates in both Nrf2-proficient and Nrf2-deficient cells; the reasons for this are unclear at present.

Similar to the Nrf2-KO A549 cells, the proportion of ATG7 within the ATG7-LC3 complex also increased in A549 cells following Nrf2 depletion by siRNA (Fig. 6E). An increase in the ATG7-LC3 conjugate levels was observed as early as one day post-transfection with si*NFE2L2* RNA. By contrast, the knockdown of Nrf2 did not affect the phosphorylation of ATG16L1 at S278 (Fig. 6E). Considering that this phosphorylated form of ATG16L1 is only present on newly forming autophagosomes [47], this result shows that new autophagosome formation proceeds normally when Nrf2 is depleted, suggesting that the observed accumulation of the ATG7/ATG3-LC3 complexes is consequent to impaired further processing due to a defect(s) at the later stage(s) of autophagy.

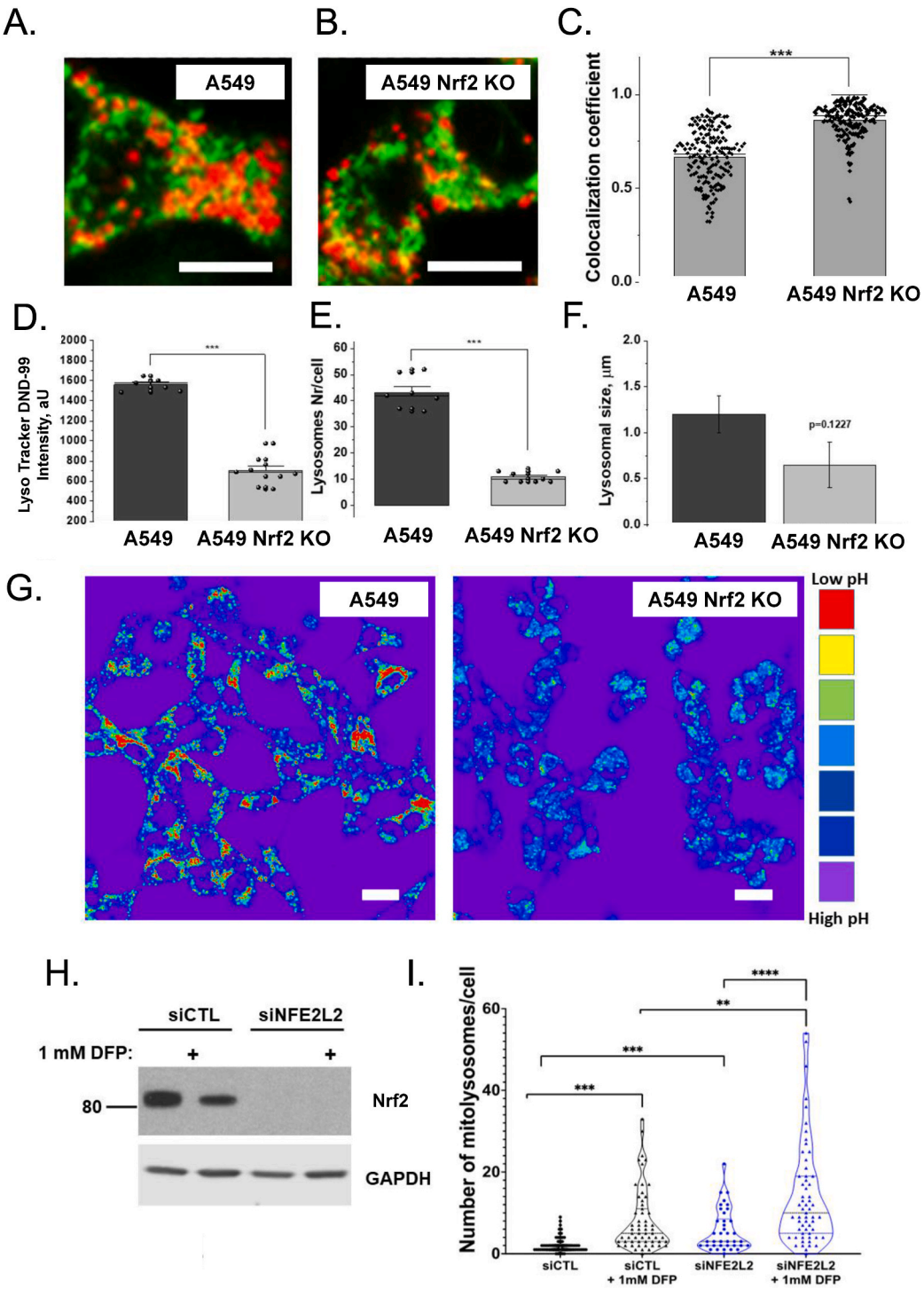

Fig. 4. The number of mitolysosomes is increased in Nrf2-deficient A549 cells. **(A,B)** Colocalization of Lyso-Tracker Red (red, lysosomes) and MitoTracker Green (green, mitochondria) in A549 **(A)** and A549 Nrf2-KO **(B)** cells. Scale bar = 10 µm. **(C)** Quantification histogram showing the levels of co-localization of LysoTracker Red with MitoTracker Green in A549 and A549 Nrf2-KO cells. Quantification bar charts depicting lysosomal staining intensity **(D),** lysosomal number **(E)** and size (**F**) in A549 and A549 Nrf2 KO cells. **(G)** Color-coded image of lysosomal staining intensity as assessed with LysoTracker Red corresponding to pH, color-to-pH scale (right). **(H)** Immunoblot of Nrf2 and GAPDH as a loading control in A549 cells stably expressing the mito-QC reporter (A549 mito-QC) transfected with 20 nM non-targeting control siRNA or *NFE2L2* siRNA for 48 h and subsequently treated without or with 1 mM deferiprone (DFP) for a further 48 h. **(I)** Quantification of the number of mitolysosomes per cell in A549 mito-QC reporter cells treated with 20 nM non-targeting control siRNA or *NFE2L2* siRNA for 48 h and subsequently treated without or with 1 mM deferiprone (DFP) for a further 24 h. Quantification was performed on fluorescence widefield images captured by Deltavision Elite microscope using the mito-QC Counter macros in ImageJ, where a threshold ratio of 0.6 with a smoothening radius of 2 was used. Data are presented as mean ± SEM. *$p < 0.05$, **$p < 0.001$, ***$p < 0.0001$. **(J,K)** Representative images of A549 mitoQC reporter cells treated with 20 nM non-targeting control siRNA **(I)** or *NFE2L2* siRNA **(J)**. The mito-QC reporter cell line consists of a mCherry-GFP tag fused to the outer mitochondrial localization signal on the protein FIS1 and works as a fluorescent pH-biosensor. When mitochondria are delivered to the lysosomes, the GFP signal is quenched and the mCherry signal is unperturbed. The mitochondria are colored in orange and the red puncta represent the mitolysosomes. Scale bar = 25 µm.

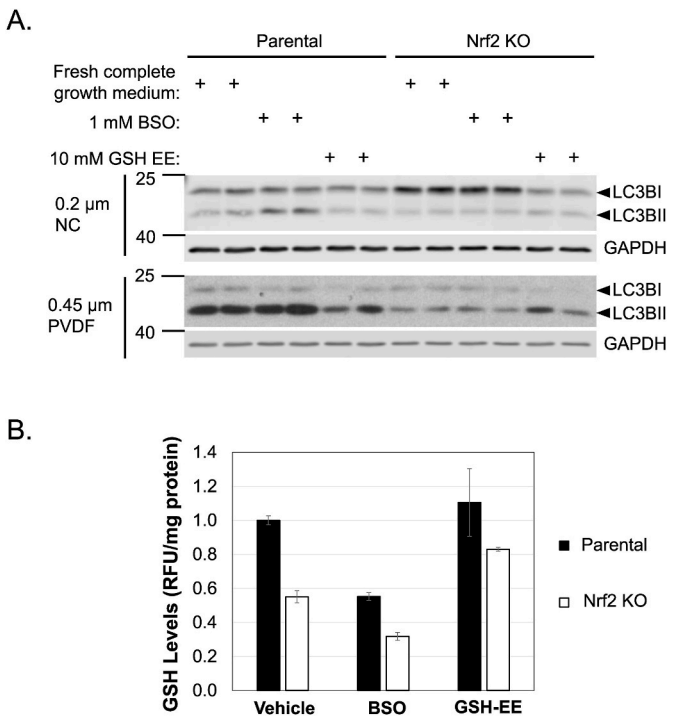

Fig. 5. Nrf2 deficiency impairs the lipidation of LC3B. (A) Western blot images of the non-lipidated (LCBI) and lipidated (LC3BII) forms of LC3B in whole-cell lysates of A549 and A549 Nrf2-KO cells treated in the presence or absence of 1 mM BSO or 10 mM GSH-EE for 20 h; GAPDH served as a loading control. **(B)** GSH measurement using the monochlorobimane probe in A549 and A549 Nrf2-KO cells treated with or without 1 mM BSO or 10 mM GSH-EE for 24 h, where relative fluorescence units (RFU) were normalized to the amount of protein in each sample.

2.8. Nrf2 deficiency increases the levels of ATG7-LC3 and ATG3-LC3 conjugates in lung cancer cells expressing mutant Keap1

To confirm that our findings are not limited to the A549 cell line, we determined the effect of Nrf2 depletion (by siRNA targeting *NFE2L2*) on the levels of ATG3, ATG7 and their respective LC3-conjugates in a panel of lung cancer cell lines. As expected, the depletion of Nrf2 caused downregulation of the Nrf2 transcriptional targets NQO1 and p62, irrespective of their corresponding basal levels, in all cell lines (Fig. 7). Similarly to A549 cells, Nrf2 depletion caused an increase, by approximately 2.5 to 3-fold for ATG7-LC3 and by approximately 2 to 5-fold for ATG7-LC3, in the conjugated forms of ATG7 and ATG3 in H460, H1944 and H1792 cells (Fig. 7A, non-reduced samples), all of which express mutant Keap1 [48,49], without affecting the total ATG7 and ATG3 levels in these cells (Fig. 7B, reduced samples). Notably however, with the exception of H520 cells, Nrf2 depletion did not affect the levels of ATG3-LC3 and ATG7-LC3 conjugates in the lung cancer cell lines H522, H1299, and CALU1, for which no mutations in Keap1 have been reported [48,49], showing that the effect of Nrf2 is particularly prominent in the context of loss-of-function Keap1 mutations.

3. Discussion

Nrf2 is frequently dysregulated in ageing and disease, rendering cells and organisms more susceptible to the negative consequences of environmental challenges, and this dysregulation is considered an important contributor to the pathogenesis of a wide range of human diseases, including Parkinson's disease, chronic obstructive pulmonary disease (COPD), nonalcoholic steatohepatitis (NASH), and diabetes mellitus [50–55]. In this study, we found that although Nrf2 deficiency decreased mitochondrial respiration, as expected, it increased the mitochondrial membrane potential, mass, DNA content, and the number of mitolysosomes per cell. The increase in mitochondrial mass and DNA in the Nrf2-KO cells was unexpected, because Nrf2 has been implicated in mitochondrial biogenesis [38]. The increase in mitolysosomes was particularly surprising, initially suggesting that mitophagy was enhanced in the absence of Nrf2, and in apparent conflict with the previously described decrease in LC3B lipidation and autophagic flux in Nrf2-deficient A549 cells [13]. Another surprising result was that the proportion of ATG7/ATG3 within their LC3B conjugates was increased. The accumulation of the ATG3-LC3B and ATG7-LC3B complexes in Nrf2-deficient cells, together with the increased number of mitolysosomes, mitochondrial mass and DNA, and the decreased LC3B lipidation, imply that mitophagy is impaired at its late stages, leading to accumulation of damaged mitochondria within mitolysosomes that cannot be efficiently degraded. This is consistent with recent findings by Anandhan et al. who, by examining the formation of LC3 puncta, reported that Nrf2 depletion in ovarian cancer cells (SKOV3) leads to an increase in LC3-positive autophagosomes and their accumulation, in part by reducing the expression of VAMP8, which mediates autophagosome-lysosome fusion [56]. Thus, the absence of Nrf2 does not affect autophagosome formation, but instead, causes an impairment at the later stage(s) of autophagy, and consequently, mitophagy.

Impaired mitolysosome processing provides a potential explanation for the accumulation of abnormal mitochondria in the livers of high-fat diet-fed Nrf2-KO mice; these mitochondria are swollen and display reduced crista and disrupted membranes [57]. Additionally, Nrf2 activation affects mitochondrial dynamics, in part by inducing the proteasomal degradation of Drp1 and thus promoting mitochondrial fusion [58]. In agreement, a recent proteomics analysis in inflammatory macrophages showed an enrichment in mitochondrial fusion with Nrf2 activation, including the mitochondrial fusion proteins, Opa1, Mfn1 and Mfn2, and a significant increase in the mitochondrial fission factors, Mff and Mief2, with Nrf2 disruption, suggesting that Nrf2 may play a role in mitochondrial adaptation during inflammation [32]. Confocal microscopy analysis of mitochondrial morphology further revealed that prolonged stimulation with lipopolysaccharide (LPS) caused a switch in mitochondrial morphology, from intermediate to fused/elongated, which was enhanced by Nrf2 activation and suppressed by Nrf2 disruption. Together, these findings highlight the critical role of Nrf2 in mitochondrial adaptation to various conditions of stress. In addition to its recognized contribution to mitochondrial biogenesis, dynamics and bioenergetics [59], the current study unveils mitolysosome processing as another way by which Nrf2 contributes to mitochondrial health.

It is notable that the effect of Nrf2 depletion was much more prominent in Keap1-mutant than Keap1-wild-type cells. A possible explanation could be that cells with mutant Keap1 are 'addicted' to the upregulation of Nrf2 and much more dependent on it than cells with wild-type Keap1. For example, the levels of GSH are expected to be higher in cells with mutant Keap1, due to the upregulation of Nrf2, and thus Nrf2 depletion would cause a much greater decrease in the GSH levels (and a corresponding increase in the level of ROS) than in cells with wild-type Keap1 and normal levels of Nrf2. Another, not mutually exclusive possibility could be that mutations in Keap1 affect its interactions not only with Nrf2, but also with its other binding partners, such as p62. It has been shown that p62 recruits Keap1 and Rbx1 to mitochondria, and the resulting p62-Keap1-Rbx1 complex ubiquitinates mitochondria in Parkin-independent mitophagy; p62 also connects mitochondria to autophagosomes through interactions with ubiquitin and LC3 [20]. Further work is needed to test these possibilities.

4. Conclusion

Collectively, our results uncover a previously unrecognized role for Nrf2 in mitochondrial health: Nrf2 facilitates mitolysosome processing thereby ensuring timely clearance of damaged mitochondria. This is particularly evident in the context of loss-of-function Keap1, where Nrf2

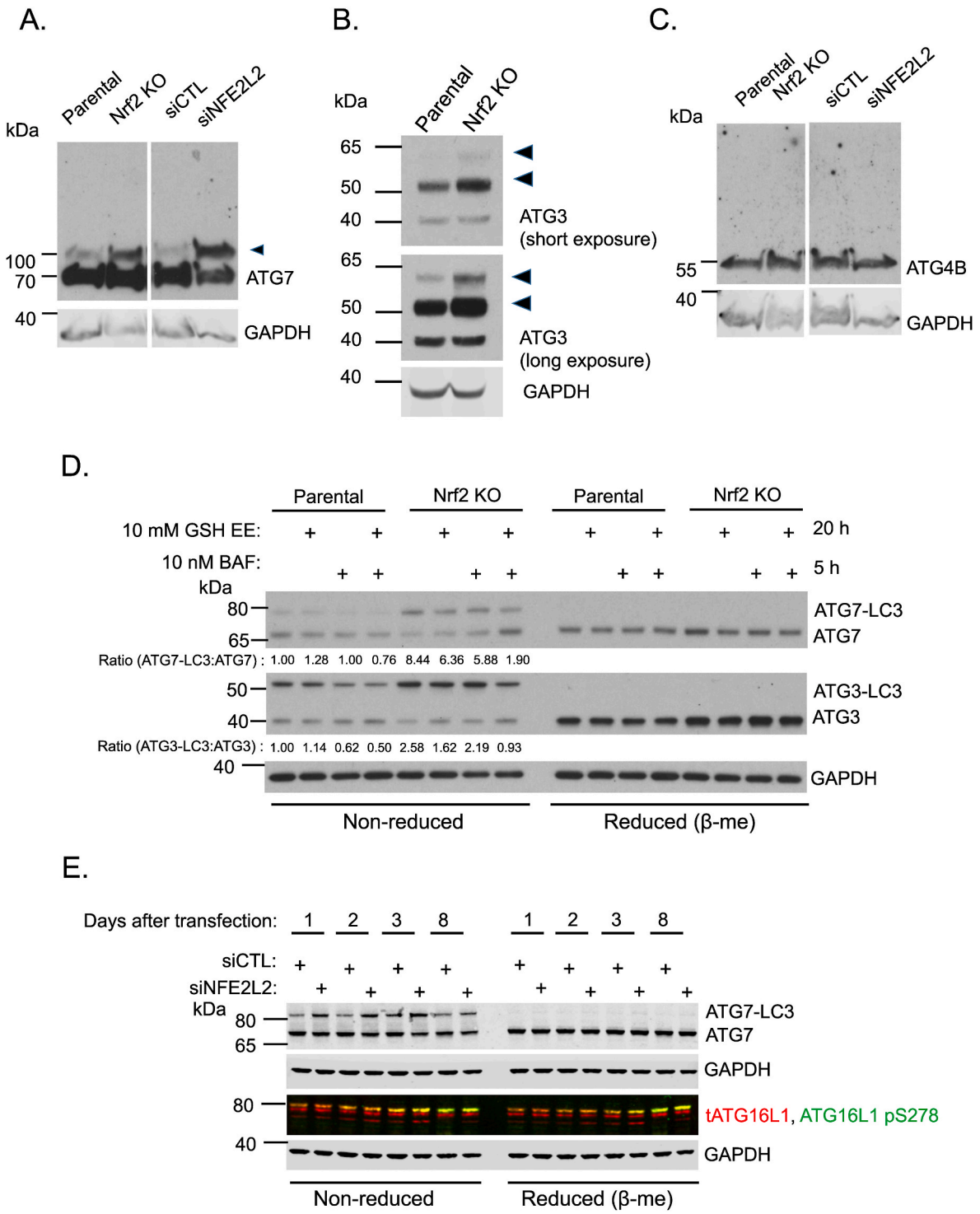

Fig. 6. Nrf2 deficiency increases the levels of ATG7-LC3 and ATG3-LC3 conjugates in A549 cells. **(A–C)** Immunoblot for ATG7 **(A)**, ATG3 **(B)** and ATG4 **(C)** of samples from the PEG-switch assay performed on lysates derived from A549, A549 Nrf2-KO and Nrf2-KD cells. Note the increase in slower migrating band(s) (marked with arrows) of ATG7 and ATG3, but not ATG4, present in the Nrf2-deficient cells. **(D)** Immunoblot of ATG7 and its LC3 conjugate and ATG3 and its LC3 conjugate in A549 and A549 Nrf2-KO cells treated with or without 10 mM GSH-EE for 20 h and in the absence or presence of 10 nM Bafilomycin for 5 h. The cell lysates were treated in the absence and presence of the reducing agent β-mercaptoethanol (β-me) to show that the covalent ATG7/ATG3-LC3 complexes can be hydrolyzed to generate the unconjugated ATG7. **(E)** Immunoblot of ATG7, its LC3 conjugate, and ATG16L (total and phosphorylated at S278; the latter is only present on newly forming autophagosomes) detected in cell lysates from siRNA-mediated transfection of A549 cell using non-targeting siRNA (siCTL) or siRNA targeting *NFE2L2* (si*NFE2L2*). GAPDH levels served as a loading control.

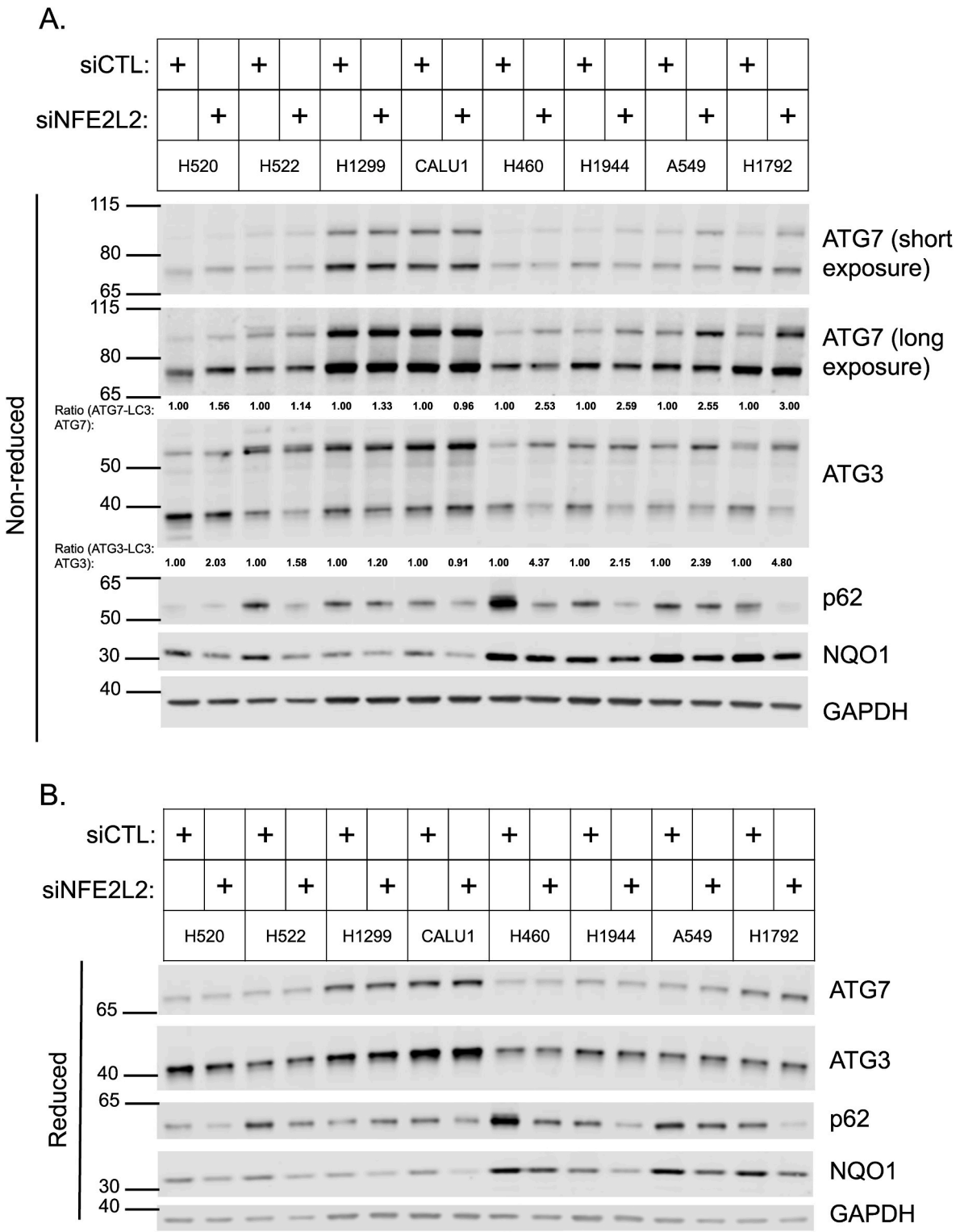

Fig. 7. Nrf2 deficiency increases the levels of ATG7-LC3 and ATG3-LC3 conjugates in lung cancer cells expressing mutant Keap1.
Immunoblots for ATG7, ATG3, p62 and NQO1 in lysates of lung cancer cells expressing wild-type Keap1 (H520, H522, H1299, CALU1) or mutant Keap1 (H460, H1944, A549 and H1792) following siRNA-mediated transfection using non-targeting siRNA (siCTL) or siRNA targeting *NFE2L2* (si*NFE2L2*) for 72 h. The cell lysates were treated in the absence **(A)** and presence of the reducing agent β-mercaptoethanol (β-me) **(B)** to show that the covalent ATG7-LC3 and ATG3-LC3 complexes can be hydrolyzed to generate the unconjugated ATG7 and ATG3. GAPDH levels served as a loading control.

is constitutively active, counteracting the oncogene-driven increase in the production of reactive oxygen species.

5. Materials and methods

5.1. Cell culture

The human lung cancer cell lines A549, CALU1, H460, H1944, H1792, H520, H522 and H1299 were obtained from the American Type Culture Collection (ATCC) where CALU1, H520 and H522 were kind gifts from C. Roland Wolf and John D. Hayes (University of Dundee). The cells were grown in Tissue Culture (TC)-treated flasks and maintained in a humidified 5% CO_2 37 °C incubator. The cell culture medium was high-glucose-Dulbecco's Modified Eagle Medium (DMEM) (Cat. 11,995,065, Thermo), supplemented with 10% heat inactivated fetal bovine serum (FBS) (Thermo). The cells were split every 3–4 days and the growth medium in the flasks was replenished every other day. Homozygous Nrf2-KO A549 cells were generated using CRISPR/Cas9 genome editing and confirmed by sequencing [30]. The cell cultures were routinely tested to ensure that they were mycoplasma-free.

5.2. RNAi transfection

A549 cells (2.5×10^5 cells per well of a 6-well plate) were reverse transfected with either 20 nM SMARTpool non-targeting siRNA control (Dharmacon) or SMARTpool siRNA targeting *NFE2L2* (Dharmacon) using 5 μL of Lipofectamine RNAiMAX (Thermo) per well of a 6-well plate following the manufacturer's instructions (Thermo). The following day, the medium was replaced with fresh complete growth medium, and the cells were collected at various time points post-transfection. For the eight- or ten-day post-transfection experiments, the transfected cells were reverse transfected at day four to maintain the knockdown. The growth medium was replenished every other day.

5.3. Western blotting

Cells were lysed in SDS lysis buffer [25 mM Tris HCL pH 6.8, 2% SDS (w/v) and 10% Glycerol (v/v)] and sonicated at 20% amplitude (Vibra-Cell™, Sonics). Bicinchoninic acid (BCA) assay (Thermo) was used to measure the protein content of the lysates according to the manufacturer's instructions. Equal amounts of protein (between 15 and 20 μg) were subjected to polyacrylamide gel electrophoresis using either the 4–12% NuPAGE (Bis-Tris) (Thermo) or 8%, 10% or 15% SDS-PAGE (Tris-Glycine) (Biorad) systems. The resolved proteins were subsequently transferred onto 0.45-μm nitrocellulose (NC) membranes using wet transfer (Biorad). When blotting for LC3, semi-dry transfer was employed using the *Trans*-blot Turbo system (Biorad), where the proteins that had been resolved on 15% SDS- polyacrylamide gels were transferred onto 0.2-μm polyvinylflouridine (PVDF) membranes to visualise the lipidated form of LC3 or transferred onto 0.45-μm NC membranes to visualise the non-lipidated form of LC3. The membranes were subsequently blocked with 5% (w/v) non-fat milk (Marvel) in phosphate buffered saline (PBS) with 0.1% (v/v) Tween-20 (PBS-T) for 30 min to 1 h at room temperature (22 °C) with constant agitation (60 rpm). Subsequently, the membranes were incubated with primary antibodies overnight at 4 °C. The primary antibodies used were: NRF2, NQO1, LC3B, ATG7, ATG4B, [1:1000, Cell Signaling Technologies (CST)], SQSTM1 (p62), ATG3, ATG16L1, ATG16L1 pS218 (1:1000, Abcam), GAPDH (1:20,000, Proteintech). After the primary antibody incubation, the membranes were washed thrice every 10 min in PBS-T and were incubated with either horseradish peroxidase (HRP)-conjugated (1:5000, CST) or fluorescently-conjugated (1:20,000, LI-COR) goat anti-mouse or anti-rabbit secondary antibodies for 1 h at room temperature (22 °C). Subsequently, the immunoblots were washed thrice with PBS-T for 30 min and were either visualized suing chemiluminescence (Thermo) or using the Odyssey CLx infrared imaging system (LI-COR). All immunoblots are representative of 2–3 independent experiments.

5.4. Extracellular flux analysis

A549 cells were trypsinised, counted and seeded in high-glucose DMEM with 10% FBS at a seeding density of 5–6 x 10^4 cells per well approximately 4 h prior to starting the experiment. Seahorse XF Assays were conducted according to the manufacturer's instructions (Agilent Technologies), where the Seahorse XF Cell Mito Stress test kit (Agilent Technologies) was used to perform the experiments using the Seahorse XFe24 Analyzer. All reagents used in this assay were obtained from Agilent Technologies. Oligomycin (1 μM), FCCP (1 μM) and rotenone/antimycin A (1 μM) were used for the experiments and the XF Cell Mito Stress Test template protocol in the Agilent Wave Software program was selected to perform the experiments.

5.5. Live cell imaging

For measurements of ΔΨm, cells plated on 22-mm glass coverslips were loaded for 30 min at room temperature with 25 nM tetramethylrhodamine methylester (TMRM; Invitrogen) in a HEPES buffered saline solution (HBSS) composed of 156 mM NaCl, 3 mM KCl, 2 mM $MgSO_4$, 1.25 mM KH_2PO_4, 2 mM $CaCl_2$, 10 mM glucose and 10 mM HEPES; pH adjusted to 7.35 with NaOH. The dye remained present in the media at the time of recording. Confocal images were obtained using a Zeiss 710 VIS CLSM equipped with a META detection system and a 40× oil immersion objective. TMRM was excited using the 560 nm laser line and fluorescence was measured above 580 nm. For basal ΔΨm measurements, Z-stack images were obtained by confocal microscopy and analysed using Zeiss software. For analysis of response to mitochondrial toxins, images were recorded continuously from a single focal plane. TMRM is used in the redistribution mode to assess ΔΨm, and therefore a reduction in TMRM fluorescence represents mitochondrial depolarization.

For measurement of mitochondrial ROS production by single-live-cell imaging, cells were pre-incubated with MitoTracker Red CM-H (2) XROS for 10 min at room temperature. MitoTracker Red CM-H (2)XROS fluorescence was measured using 560 nm excitation and emission above 580 nm. For measurement of total ROS levels in cell populations, A549 cells were incubated with 10 μM of H_2DCFDA in HBSS. The levels of ROS were determined by measuring the fluorescence emitted by live cells, using a fluorometer (Ex485/Em538), and the fluorescence was normalized for the amount of total protein.

5.6. Measurement of NADH/FAD redox indices and pools, and NADPH

NADH autofluorescence was measured using an epifluorescence inverted microscope equipped with a 20*X* fluorite objective. Excitation light at a wavelength of 350 nm was provided by a Xenon arc lamp, the beam passing through a monochromator (Cairn Research, Kent, UK). Emitted fluorescence light was reflected through a 455 nm long-pass filter to a cooled CCD camera (Retiga, QImaging, Canada) and digitized to 12-bit resolution. Imaging data were collected and analysed using software from Andor (Belfast, UK). FAD autofluorescence was monitored using a Zeiss 710 VIS CLSM equipped with a META detection system and a 40× oil immersion objective. Excitation was using the 454 nm Argon laser line and fluorescence was measured from 505 to 550 nm. Illumination intensity was kept to a minimum (at 0.1–0.2% of laser output) to avoid phototoxicity and the pinhole set to give an optical slice of ~2 μm. FAD and NADH redox indexes and mitochondrial pools were estimated as described [60].

5.7. Reduced glutathione (GSH) assessment

For single live-cell imaging experiments, cells were incubated with

50 μM monochlorobimane (MCB) (Molecular Probes, Invitrogen) for 40 min in HEPES buffered salt solution prior to imaging. Cells were then washed with HEPES buffered salt solution and images of the fluorescence of the MCB-GSH were acquired using a Zeiss 710 CLSM with excitation at 405 nm and emission at 435–485 nm. The levels of GSH were also determined in cell populations following incubation with MCB in HBSS; the resulting fluorescence was measured using a fluorometer (Ex390nm/Em490) and normalized for total protein.

5.8. Assessment of mitochondrial and lysosomal co-localization

For identification of mitochondrial and lysosomal co-localization, cells were loaded with 200 nM MitoTracker Green FM and 50 nM LysoTracker Red in HBSS for 30 min before experiments. Confocal images were obtained using a Zeiss 710 confocal microscope equipped with 40*X* oil immersion objective. The 488 nm argon laser line was used to excite MitoTracker Green fluorescence which was measured between 505 and 530 nm. Illumination intensity was kept to a minimum (about 1% of laser output) to avoid phototoxicity and the pinhole set to give an optical slice of ~2 μm. For LysoTracker Red, the 543 nm Ne/He laser line was used with measurement above 650 nm. All data presented were obtained from at least 5 coverslips and 2–3 different cell preparations.

5.9. mtDNA content assessment

Mitochondrial DNA (mtDNA) content in live cells was assessed using Quant-iT PicoGreen dsDNA probe (Molecular Probes Inc.) at 3 μM directly into the cell culture medium. The cells were incubated for 30 min, under standard cell culture conditions (37 °C, 5% CO_2). The cells were then rinsed 3*X* in pre-warmed HBSS and visualized using a Zeiss 710 VIS CLSM equipped with a META detection system under 40 × magnification. Excitation was using the 488 nm Argon laser line and fluorescence was measured from 510 to 550 nm.

5.10. Mito-QC reporter assay

A549^{MGFIS1} cells, generated as described [40], were reverse transfected with 20 nM of non-targeting or *NFE2L2* siRNA for 72 h and grown on glass coverslips (1.5-mm thickness). Forty-eight hours post-transfection, positive control for mitophagy induction cells were treated with 1 mM DFP for 24 h. On the next day, 3.7% PFA was dissolved in PBS (pH 7.25) for 10 min at room temperature (22 °C) (RT), the cells were washed thrice with PBS, fixed and stained with 1 μg/ml DAPI for 5 min at RT. The coverslips were washed once with PBS, mounted on glass slides with anti-fade prolong gold mounting medium (Thermo) and cured overnight at RT in the dark. The images were collected with the widefield microscope Deltavision Elite using the Softworx software for image acquisition where 40 × magnification was used. Images were acquired in both the green fluorescent protein (GFP) and mCherry channels. Images of least 45 cells were captured and analysed. The mQC counter plugin was used on ImageJ to quantify the number of mitolysosomes per cell. The protocol was adapted from Montava-Garriga et al. [61].

5.11. PEG-switch assay

Twenty-four hours after seeding 6×10^5 A549 cells in each well of a six-well plate, the cells were washed twice with DPBS and lysed immediately in 200 μL of alkylating buffer (100 mM Tris HCl pH 7.4, 1% SDS, 100 mM maleimide). The lysates were incubated at 50 °C with vigorous shaking (1200 rpm) for 25 min. Subsequently, the lysates were passed through a Qiashredder column (Qiagen) to shear the DNA (16,900 g for 2 min). The protein concentrations of the lysates were measured and adjusted with the alkylating buffer to ensure equal amounts of protein between the lysates. The samples (130 μL) in each tube were transferred into 0.5 ml zeba-spin desalting columns (Thermo) to remove free maleimide. The reducing agent dithiothreitol (DTT) was added at a final concentration of 50 mM to the eluates, and the samples were incubated at 25 °C for 20 min. The samples in each tube were transferred into 0.5 ml zeba-spin desalting columns to remove free DTT. The reduced and desalted samples were incubated in a labelling buffer containing PEG (5000) (Sigma) at final concentration of 2 mM PEG (5000)-maleimide, 0.5% SDS and 100 mM Tris HCl pH 7.4 for 2 h at 25 °C to label the reversibly oxidised amino acids. To quench the reaction, 100 mM of maleimide was added, and the samples were incubated at 22 °C for 10 min. Subsequently, 1 part of 5X loading buffer (250 mM Tris HCl pH 6.8, 20% glycerol (v/v), 4% SDS (w/v), 0.001% bromophenol blue (w/v)) was added to 4 parts of the lysate. The lysates were then subjected to either NuPAGE/Bis-Tris or Tris/Glycine SDS-polyacrylamide gel electrophoresis and western blotting. This protocol was adapted from Burgoyne et al. [45].

5.12. Statistical analysis

Data analysis of live cell images was performed using Origin Pro 2019 (MicroCal Software Inc. Northampton, MA) software. Student's t-tests were performed using GraphPad Prism v8.0 or v9.0 software (GraphPad Software, Inc. La Jolla, USA). Differences were considered statistically significant with p-value <0.05. Results are expressed as mean value ± SEM.

Author contribution

A.T.D.-K. S.D.N. P.R.A. and A.Y.A. conceived the project, designed the experiments, contributed to data interpretation and writing of the manuscript. S.D.N. P.R.A. E.V·K, C.L, and M.N. performed experiments, data analysis and interpretation. L.d.l.V. produced Nrf2-knockout A549 cells. I.G.G. produced the A549MGFIS1 reporter cell line. All authors reviewed and edited the manuscript before submission.

Declaration of competing interests

The authors declare that they have no known competing financial interests or personal relationships that could have appeared to influence the work reported in this paper.

Acknowledgments

We thank Reata Pharmaceuticals, Tenovus Scotland (T19/30), and the Biotechnology and Biological Sciences Research Council (BB/T017546/1 and BB/T508111/1) for supporting our research. The work described in this article is facilitated by collaboration through COST Action CA20121, supported by the European Cooperation in Science and Technology (www.cost.eu) (https://benbedphar.org/about-benbedphar/).

References

[1] M. Yamamoto, T.W. Kensler, H. Motohashi, The KEAP1-NRF2 system: a thiol-based sensor-effector apparatus for maintaining redox homeostasis, Physiol. Rev. 98 (3) (2018) 1169–1203.
[2] J.D. Hayes, A.T. Dinkova-Kostova, The Nrf2 regulatory network provides an interface between redox and intermediary metabolism, Trends Biochem. Sci. 39 (4) (2014) 199–218.
[3] S.B. Cullinan, J.D. Gordan, J. Jin, J.W. Harper, J.A. Diehl, The Keap1-BTB protein is an adaptor that bridges Nrf2 to a Cul3-based E3 ligase: oxidative stress sensing by a Cul3-Keap1 ligase, Mol. Cell Biol. 24 (19) (2004) 8477–8486.
[4] A. Kobayashi, M.I. Kang, H. Okawa, M. Ohtsuji, Y. Zenke, T. Chiba, K. Igarashi, M. Yamamoto, Oxidative stress sensor Keap1 functions as an adaptor for Cul3-based E3 ligase to regulate proteasomal degradation of Nrf2, Mol. Cell Biol. 24 (16) (2004) 7130–7139.
[5] D.D. Zhang, S.C. Lo, J.V. Cross, D.J. Templeton, M. Hannink, Keap1 is a redox-regulated substrate adaptor protein for a Cul3-dependent ubiquitin ligase complex, Mol. Cell Biol. 24 (24) (2004) 10941–10953.
[6] A.T. Dinkova-Kostova, W.D. Holtzclaw, R.N. Cole, K. Itoh, N. Wakabayashi, Y. Katoh, M. Yamamoto, P. Talalay, Direct evidence that sulfhydryl groups of

Keap1 are the sensors regulating induction of phase 2 enzymes that protect against carcinogens and oxidants, Proc. Natl. Acad. Sci. U. S. A. 99 (18) (2002) 11908–11913.
[7] A.T. Dinkova-Kostova, I.M. Copple, Advances and challenges in therapeutic targeting of NRF2, Trends Pharmacol. Sci. 44 (3) (2023) 137–149.
[8] A. Cuadrado, A.I. Rojo, G. Wells, J.D. Hayes, S.P. Cousin, W.L. Rumsey, O. C. Attucks, S. Franklin, A.L. Levonen, T.W. Kensler, A.T. Dinkova-Kostova, Therapeutic targeting of the NRF2 and KEAP1 partnership in chronic diseases, Nature reviews, Drug Discov. 18(4) (2019) 295–317.
[9] A. Cuadrado, M. Pajares, C. Benito, J. Jimenez-Villegas, M. Escoll, R. Fernandez-Gines, A.J.G. Yague, D. Lastra, G. Manda, A.I. Rojo, A.T. Dinkova-Kostova, Can activation of NRF2 Be a strategy COVID-19? Trends Pharmacol. Sci. 41 (9) (2020) 598–610.
[10] S. Dayalan Naidu, A.T. Dinkova-Kostova, Omaveloxolone (Skyclarys(TM)) for patients with Friedreich's ataxia, Trends Pharmacol. Sci. 44 (6) (2023) 394–395.
[11] K.M. Holmstrom, L. Baird, Y. Zhang, I. Hargreaves, A. Chalasani, J.M. Land, L. Stanyer, M. Yamamoto, A.T. Dinkova-Kostova, A.Y. Abramov, Nrf2 impacts cellular bioenergetics by controlling substrate availability for mitochondrial respiration, Biol. open 2 (8) (2013) 761–770.
[12] M.H. Ludtmann, P.R. Angelova, Y. Zhang, A.Y. Abramov, A.T. Dinkova-Kostova, Nrf2 affects the efficiency of mitochondrial fatty acid oxidation, Biochem. J. 457 (3) (2014) 415–424.
[13] E.V. Knatko, M.H. Tatham, Y. Zhang, C. Castro, M. Higgins, S. Dayalan Naidu, C. Leonardi, L. de la Vega, T. Honda, J.L. Griffin, R.T. Hay, A.T. Dinkova-Kostova, Downregulation of Keap1 confers features of a fasted metabolic state, iScience 23 (10) (2020) 101638.
[14] M. Komatsu, H. Kurokawa, S. Waguri, K. Taguchi, A. Kobayashi, Y. Ichimura, Y. S. Sou, I. Ueno, A. Sakamoto, K.I. Tong, M. Kim, Y. Nishito, S. Iemura, T. Natsume, T. Ueno, E. Kominami, H. Motohashi, K. Tanaka, M. Yamamoto, The selective autophagy substrate p62 activates the stress responsive transcription factor Nrf2 through inactivation of Keap1, Nat. Cell Biol. 12 (3) (2010) 213–223.
[15] A. Jain, T. Lamark, E. Sjottem, K.B. Larsen, J.A. Awuh, A. Overvatn, M. McMahon, J.D. Hayes, T. Johansen, p62/SQSTM1 is a target gene for transcription factor NRF2 and creates a positive feedback loop by inducing antioxidant response element-driven gene transcription, J. Biol. Chem. 285 (29) (2010) 22576–22591.
[16] M. Pajares, N. Jimenez-Moreno, A.J. Garcia-Yague, M. Escoll, M.L. de Ceballos, F. Van Leuven, A. Rabano, M. Yamamoto, A.I. Rojo, A. Cuadrado, Transcription factor NFE2L2/NRF2 is a regulator of macroautophagy genes, Autophagy 12 (10) (2016) 1902–1916.
[17] M. Pajares, A.I. Rojo, E. Arias, A. Diaz-Carretero, A.M. Cuervo, A. Cuadrado, Transcription factor NFE2L2/NRF2 modulates chaperone-mediated autophagy through the regulation of LAMP2A, Autophagy 14 (8) (2018) 1310–1322.
[18] S. Dayalan Naidu, D. Dikovskaya, E. Gaurilcikaite, E.V. Knatko, Z.R. Healy, H. Mohan, G. Koh, A. Laurell, G. Ball, D. Olagnier, L. de la Vega, I.G. Ganley, P. Talalay, A.T. Dinkova-Kostova, Transcription factors NRF2 and HSF1 have opposing functions in autophagy, Sci. Rep. 7 (1) (2017) 11023.
[19] D. Olagnier, R.R. Lababidi, S.B. Hadj, A. Sze, Y. Liu, S.D. Naidu, M. Ferrari, Y. Jiang, C. Chiang, V. Beljanski, M.L. Goulet, E.V. Knatko, A.T. Dinkova-Kostova, J. Hiscott, R. Lin, Activation of Nrf2 signaling augments vesicular stomatitis virus oncolysis via autophagy-driven suppression of antiviral immunity, Mol. Ther. 25 (8) (2017) 1900–1916.
[20] T. Yamada, D. Murata, Y. Adachi, K. Itoh, S. Kameoka, A. Igarashi, T. Kato, Y. Araki, R.L. Huganir, T.M. Dawson, T. Yanagawa, K. Okamoto, M. Iijima, H. Sesaki, Mitochondrial stasis reveals p62-mediated ubiquitination in parkin-independent mitophagy and mitigates nonalcoholic fatty liver disease, Cell Metabol. 28 (4) (2018) 588–604, e5.
[21] T. Yamada, T.M. Dawson, T. Yanagawa, M. Iijima, H. Sesaki, SQSTM1/p62 promotes mitochondrial ubiquitination independently of PINK1 and PRKN/parkin in mitophagy, Autophagy 15 (11) (2019) 2012–2018.
[22] H.C. Bertrand, M. Schaap, L. Baird, N.D. Georgakopoulos, A. Fowkes, C. Thiollier, H. Kachi, A.T. Dinkova-Kostova, G. Wells, Design, synthesis, and evaluation of triazole derivatives that induce Nrf2 dependent gene products and inhibit the keap1-nrf2 protein-protein interaction, J. Med. Chem. 58 (18) (2015) 7186–7194.
[23] D.A. East, F. Fagiani, J. Crosby, N.D. Georgakopoulos, H. Bertrand, M. Schaap, A. Fowkes, G. Wells, M. Campanella, PMI: a DeltaPsi independent pharmacological regulator of mitophagy, Chem. Biol. 21 (11) (2014) 1585–1596.
[24] N.D. Georgakopoulos, M. Frison, M.S. Alvarez, H. Bertrand, G. Wells, M. Campanella, Reversible Keap1 inhibitors are preferential pharmacological tools to modulate cellular mitophagy, Sci. Rep. 7 (1) (2017) 10303.
[25] N.D. Georgakopoulos, G. Wells, M. Campanella, The pharmacological regulation of cellular mitophagy, Nat. Chem. Biol. 13 (2) (2017) 136–146.
[26] Y. Ichimura, T. Kirisako, T. Takao, Y. Satomi, Y. Shimonishi, N. Ishihara, N. Mizushima, I. Tanida, E. Kominami, M. Ohsumi, T. Noda, Y. Ohsumi, A ubiquitin-like system mediates protein lipidation, Nature 408 (6811) (2000) 488–492.
[27] K. Frudd, T. Burgoyne, J.R. Burgoyne, Oxidation of Atg3 and Atg7 mediates inhibition of autophagy, Nat. Commun. 9 (1) (2018) 95.
[28] N. Cancer Genome Atlas Research, Comprehensive molecular profiling of lung adenocarcinoma, Nature 511 (7511) (2014) 543–550.
[29] J.D. Hayes, A.T. Dinkova-Kostova, K.D. Tew, Oxidative stress in cancer, Cancer Cell 38 (2) (2020) 167–197.
[30] J.R. Murray, L. de la Vega, J.D. Hayes, L. Duan, T.M. Penning, Induction of the antioxidant response by the transcription factor NRF2 increases bioactivation of the mutagenic air pollutant 3-nitrobenzanthrone in human lung cells, Chem. Res. Toxicol. 32 (12) (2019) 2538–2551.
[31] A. Singh, V. Misra, R.K. Thimmulappa, H. Lee, S. Ames, M.O. Hoque, J.G. Herman, S.B. Baylin, D. Sidransky, E. Gabrielson, M.V. Brock, S. Biswal, Dysfunctional KEAP1-NRF2 interaction in non-small-cell lung cancer, PLoS Med. 3 (10) (2006) e420.
[32] D.G. Ryan, E.V. Knatko, A.M. Casey, J.L. Hukelmann, S. Dayalan Naidu, A. J. Brenes, T. Ekkunagul, C. Baker, M. Higgins, L. Tronci, E. Nikitopolou, T. Honda, R.C. Hartley, L.A.J. O'Neill, C. Frezza, A.I. Lamond, A.Y. Abramov, J.S.C. Arthur, D.A. Cantrell, M.P. Murphy, A.T. Dinkova-Kostova, Nrf2 activation reprograms macrophage intermediary metabolism and suppresses the type I interferon response, iScience 25 (2) (2022) 103827.
[33] A.Y. Abramov, T.K. Smulders-Srinivasan, D.M. Kirby, R. Acin-Perez, J.A. Enriquez, R.N. Lightowlers, M.R. Duchen, D.M. Turnbull, Mechanism of neurodegeneration of neurons with mitochondrial DNA mutations, Brain 133 (Pt 3) (2010) 797–807.
[34] N. Esteras, J.D. Rohrer, J. Hardy, S. Wray, A.Y. Abramov, Mitochondrial hyperpolarization in iPSC-derived neurons from patients of FTDP-17 with 10+16 MAPT mutation leads to oxidative stress and neurodegeneration, Redox Biol. 12 (2017) 410–422.
[35] O. Vergun, T.V. Votyakova, I.J. Reynolds, Spontaneous changes in mitochondrial membrane potential in single isolated brain mitochondria, Biophys. J. 85 (5) (2003) 3358–3366.
[36] P.R. Angelova, A.Y. Abramov, Functional role of mitochondrial reactive oxygen species in physiology, Free Radic. Biol. Med. 100 (2016) 81–85.
[37] S. Kovac, P.R. Angelova, K.M. Holmstrom, Y. Zhang, A.T. Dinkova-Kostova, A. Y. Abramov, Nrf2 regulates ROS production by mitochondria and NADPH oxidase, Biochim. Biophys. Acta 1850 (4) (2014) 794–801.
[38] A.D. Cherry, C.A. Piantadosi, Regulation of mitochondrial biogenesis and its intersection with inflammatory responses, Antioxidants Redox Signal. 22 (12) (2015) 965–976.
[39] A.V. Berezhnov, M.P. Soutar, E.I. Fedotova, M.S. Frolova, H. Plun-Favreau, V. P. Zinchenko, A.Y. Abramov, Intracellular pH modulates autophagy and mitophagy, J. Biol. Chem. 291 (16) (2016) 8701–8708.
[40] G.F. Allen, R. Toth, J. James, I.G. Ganley, Loss of iron triggers PINK1/Parkin-independent mitophagy, EMBO Rep. 14 (12) (2013) 1127–1135.
[41] D.J. Klionsky, A.K. Abdel-Aziz, S. Abdelfatah, M. Abdellatif, A. Abdoli, S. Abel, H. Abeliovich, M.H. Abildgaard, Y.P. Abudu, A. Acevedo-Arozena, I. E. Adamopoulos, K. Adeli, T.E. Adolph, A. Adornetto, E. Aflaki, G. Agam, A. Agarwal, B.B. Aggarwal, M. Agnello, P. Agostinis, J.N. Agrewala, A. Agrotis, P. V. Aguilar, S.T. Ahmad, Z.M. Ahmed, U. Ahumada-Castro, S. Aits, S. Aizawa, Y. Akkoc, T. Akoumianaki, H.A. Akpinar, A.M. Al-Abd, L. Al-Akra, A. Al-Gharaibeh, M.A. Alaoui-Jamali, S. Alberti, E. Alcocer-Gomez, C. Alessandri, M. Ali, M.A. Alim Al-Bari, S. Aliwaini, J. Alizadeh, E. Almacellas, A. Almasan, A. Alonso, G.D. Alonso, N. Altan-Bonnet, D.C. Altieri, E.M.C. Alvarez, S. Alves, C. Alves da Costa, M. M. Alzaharna, M. Amadio, C. Amantini, C. Amaral, S. Ambrosio, A.O. Amer, V. Ammanathan, Z. An, S.U. Andersen, S.A. Andrabi, M. Andrade-Silva, A. M. Andres, S. Angelini, D. Ann, U.C. Anozie, M.Y. Ansari, P. Antas, A. Antebi, Z. Anton, T. Anwar, L. Apetoh, N. Apostolova, T. Araki, Y. Araki, K. Arasaki, W. L. Araujo, J. Araya, C. Arden, M.A. Arevalo, S. Arguelles, E. Arias, J. Arikkath, H. Arimoto, A.R. Ariosa, D. Armstrong-James, L. Arnaune-Pelloquin, A. Aroca, D. S. Arroyo, I. Arsov, R. Artero, D.M.L. Asaro, M. Aschner, M. Ashrafizadeh, O. Ashur-Fabian, A.G. Atanasov, A.K. Au, P. Auberger, H.W. Auner, L. Aurelian, R. Autelli, L. Avagliano, Y. Avalos, S. Aveic, C.A. Aveleira, T. Avin-Wittenberg, Y. Aydin, S. Ayton, S. Ayyadevara, M. Azzopardi, M. Baba, J.M. Backer, S. K. Backues, D.H. Bae, O.N. Bae, S.H. Bae, E.H. Baehrecke, A. Baek, S.H. Baek, S. H. Baek, G. Bagetta, A. Bagniewska-Zadworna, H. Bai, J. Bai, X. Bai, Y. Bai, N. Bairagi, S. Baksi, T. Balbi, C.T. Baldari, W. Balduini, A. Ballabio, M. Ballester, S. Balazadeh, R. Balzan, R. Bandopadhyay, S. Banerjee, S. Banerjee, A. Banreti, Y. Bao, M.S. Baptista, A. Baracca, C. Barbati, A. Bargiela, D. Barila, P.G. Barlow, S. J. Barmada, E. Barreiro, G.E. Barreto, J. Bartek, B. Bartel, A. Bartolome, G.R. Barve, S.H. Basagoudanavar, D.C. Bassham, R.C. Bast Jr., A. Basu, H. Batoko, I. Batten, E. E. Baulieu, B.L. Baumgarner, J. Bayry, R. Beale, I. Beau, F. Beaumatin, L.R. G. Bechara, G.R. Beck Jr., M.F. Beers, J. Begun, C. Behrends, G.M.N. Behrens, R. Bei, E. Bejarano, S. Bel, C. Behl, A. Belaid, N. Belgareh-Touze, C. Bellarosa, F. Belleudi, M. Bello Perez, R. Bello-Morales, J.S.O. Beltran, S. Beltran, D. M. Benbrook, M. Bendorius, B.A. Benitez, I. Benito-Cuesta, J. Bensalem, M. W. Berchtold, S. Berezowska, D. Bergamaschi, M. Bergami, A. Bergmann, L. Berliocchi, C. Berlioz-Torrent, A. Bernard, L. Berthoux, C.G. Besirli, S. Besteiro, V.M. Betin, R. Beyaert, J.S. Bezbradica, K. Bhaskar, I. Bhatia-Kissova, R. Bhattacharya, S. Bhattacharya, S. Bhattacharyya, M.S. Bhuiyan, S.K. Bhutia, L. Bi, X. Bi, T.J. Biden, K. Bijian, V.A. Billes, N. Binart, C. Bincoletto, A. B. Birgisdottir, G. Bjorkoy, G. Blanco, A. Blas-Garcia, J. Blasiak, R. Blomgran, K. Blomgren, J.S. Blum, E. Boada-Romero, M. Boban, K. Boesze-Battaglia, P. Boeuf, B. Boland, P. Bomont, P. Bonaldo, S.R. Bonam, L. Bonfili, J.S. Bonifacino, B. A. Boone, M.D. Bootman, M. Bordi, C. Borner, B.C. Bornhauser, G. Borthakur, J. Bosch, S. Bose, L.M. Botana, J. Botas, C.M. Boulanger, M.E. Boulton, M. Bourdenx, B. Bourgeois, N.M. Bourke, G. Bousquet, P. Boya, P.V. Bozhkov, L.H. M. Bozi, T.O. Bozkurt, D.E. Brackney, C.H. Brandts, R.J. Braun, G.H. Braus, R. Bravo-Sagua, J.M. Bravo-San Pedro, P. Brest, M.A. Bringer, A. Briones-Herrera, V.C. Broaddus, P. Brodersen, J.L. Brodsky, S.L. Brody, P.G. Bronson, J. M. Bronstein, C.N. Brown, R.E. Brown, P.C. Brum, J.H. Brumell, N. Brunetti-Pierri, D. Bruno, R.J. Bryson-Richardson, C. Bucci, C. Buchrieser, M. Bueno, L.E. Buitrago-Molina, S. Buraschi, S. Buch, J.R. Buchan, E.M. Buckingham, H. Budak, M. Budini, G. Bultynck, F. Burada, J.R. Burgoyne, M.I. Buron, V. Bustos, S. Buttner, E. Butturini, A. Byrd, I. Cabas, S. Cabrera-Benitez, K. Cadwell, J. Cai, L. Cai, Q. Cai, M. Cairo, J.A. Calbet, G.A. Caldwell, K.A. Caldwell, J.A. Call, R. Calvani, A. C. Calvo, M. Calvo-Rubio Barrera, N.O. Camara, J.H. Camonis, N. Camougrand, M. Campanella, E.M. Campbell, F.X. Campbell-Valois, S. Campello, I. Campesi, J.

C. Campos, O. Camuzard, J. Cancino, D. Candido de Almeida, L. Canesi, I. Caniggia, B. Canonico, C. Canti, B. Cao, M. Caraglia, B. Carames, E.H. Carchman, E. Cardenal-Munoz, C. Cardenas, L. Cardenas, S.M. Cardoso, J.S. Carew, G.F. Carle, G. Carleton, S. Carloni, D. Carmona-Gutierrez, L.A. Carneiro, O. Carnevali, J. M. Carosi, S. Carra, A. Carrier, L. Carrier, B. Carroll, A.B. Carter, A.N. Carvalho, M. Casanova, C. Casas, J. Casas, C. Cassioli, E.F. Castillo, K. Castillo, S. Castillo-Lluva, F. Castoldi, M. Castori, A.F. Castro, M. Castro-Caldas, J. Castro-Hernandez, S. Castro-Obregon, S.D. Catz, C. Cavadas, F. Cavaliere, G. Cavallini, M. Cavinato, M.L. Cayuela, P. Cebollada Rica, V. Cecarini, F. Cecconi, M. Cechowska-Pasko, S. Cenci, V. Ceperuelo-Mallafre, J.J. Cerqueira, J.M. Cerutti, D. Cervia, V. B. Cetintas, S. Cetrullo, H.J. Chae, A.S. Chagin, C.Y. Chai, G. Chakrabarti, O. Chakrabarti, T. Chakraborty, T. Chakraborty, M. Chami, G. Chamilos, D. W. Chan, E.Y.W. Chan, E.D. Chan, H.Y.E. Chan, H.H. Chan, H. Chan, M.T.V. Chan, Y.S. Chan, P.K. Chandra, C.P. Chang, C. Chang, H.C. Chang, K. Chang, J. Chao, T. Chapman, N. Charlet-Berguerand, S. Chatterjee, S.K. Chaube, A. Chaudhary, S. Chauhan, E. Chaum, F. Checler, M.E. Cheetham, C.S. Chen, G.C. Chen, J.F. Chen, L.L. Chen, L. Chen, L. Chen, M. Chen, M.K. Chen, N. Chen, Q. Chen, R.H. Chen, S. Chen, W. Chen, W. Chen, X.M. Chen, X.W. Chen, X. Chen, Y. Chen, Y.G. Chen, Y. Chen, Y. Chen, Y.J. Chen, Y.Q. Chen, Z.S. Chen, Z. Chen, Z.H. Chen, Z.J. Chen, Z. Chen, H. Cheng, J. Cheng, S.Y. Cheng, W. Cheng, X. Cheng, X.T. Cheng, Y. Cheng, Z. Cheng, Z. Chen, H. Cheong, J.K. Cheong, B.V. Chernyak, S. Cherry, C. F.R. Cheung, C.H.A. Cheung, K.H. Cheung, E. Chevet, R.J. Chi, A.K.S. Chiang, F. Chiaradonna, R. Chiarelli, M. Chiariello, N. Chica, S. Chiocca, M. Chiong, S. H. Chiou, A.I. Chiramel, V. Chiurchiu, D.H. Cho, S.K. Choe, A.M.K. Choi, M.E. Choi, K.R. Choudhury, N.S. Chow, C.T. Chu, J.P. Chua, J.J.E. Chua, H. Chung, K. P. Chung, S. Chung, S.H. Chung, Y.L. Chung, V. Cianfanelli, I.A. Ciechomska, M. Cifuentes, L. Cinque, S. Cirak, M. Cirone, M.J. Clague, R. Clarke, E. Clementi, E. M. Coccia, P. Codogno, E. Cohen, M.M. Cohen, T. Colasanti, F. Colasuonno, R. A. Colbert, A. Colell, M. Colic, N.S. Coll, M.O. Collins, M.I. Colombo, D.A. Colon-Ramos, L. Combaret, S. Comincini, M.R. Cominetti, A. Consiglio, A. Conte, F. Conti, V.R. Contu, M.R. Cookson, K.M. Coombs, I. Coppens, M.T. Corasaniti, D.P. Corkery, N. Cordes, K. Cortese, M.D.C. Costa, S. Costantino, P. Costelli, A. Coto-Montes, P. J. Crack, J.L. Crespo, A. Criollo, V. Crippa, R. Cristofani, T. Csizmadia, A. Cuadrado, B. Cui, J. Cui, Y. Cui, Y. Cui, E. Culetto, A.C. Cumino, A.V. Cybulsky, M.J. Czaja, S.J. Czuczwar, S. D'Adamo, M. D'Amelio, D. D'Arcangelo, A. C. D'Lugos, G. D'Orazi, J.A. da Silva, H.S. Dafsari, R.K. Dagda, Y. Dagdas, M. Daglia, X. Dai, Y. Dai, Y. Dai, J. Dal Col, P. Dalhaimer, L. Dalla Valle, T. Dallenga, G. Dalmasso, M. Damme, I. Dando, N.P. Dantuma, A.L. Darling, H. Das, S. Dasarathy, S.K. Dasari, S. Dash, O. Daumke, A.N. Dauphinee, J.S. Davies, V.A. Davila, R.J. Davis, T. Davis, S. Dayalan Naidu, F. De Amicis, K. De Bosscher, F. De Felice, L. De Franceschi, C. De Leonibus, M.G. de Mattos Barbosa, G.R.Y. De Meyer, A. De Milito, C. De Nunzio, C. De Palma, M. De Santi, C. De Virgilio, D. De Zio, J. Debnath, B.J. DeBosch, J.P. Decuypere, M.A. Deehan, G. Deflorian, J. DeGregori, B. Dehay, G. Del Rio, J.R. Delaney, L.M.D. Delbridge, E. Delorme-Axford, M.V. Delpino, F. Demarchi, V. Dembitz, N.D. Demers, H. Deng, Z. Deng, J. Dengjel, P. Dent, D. Denton, M.L. DePamphilis, C.J. Der, V. Deretic, A. Descoteaux, L. Devis, S. Devkota, O. Devuyst, G. Dewson, M. Dharmasivam, R. Dhiman, D. di Bernardo, M. Di Cristina, F. Di Domenico, P. Di Fazio, A. Di Fonzo, G. Di Guardo, G.M. Di Guglielmo, L. Di Leo, C. Di Malta, A. Di Nardo, M. Di Rienzo, F. Di Sano, G. Diallinas, J. Diao, G. Diaz-Araya, I. Diaz-Laviada, J.M. Dickinson, M. Diederich, M. Dieude, I. Dikic, S. Ding, W.X. Ding, L. Dini, J. Dinic, M. Dinic, A. T. Dinkova-Kostova, M.S. Dionne, J.H.W. Distler, A. Diwan, I.M.C. Dixon, M. Djavaheri-Mergny, I. Dobrinski, O. Dobrovinskaya, R. Dobrowolski, R.C. J. Dobson, J. Dokic, S. Dokmeci Emre, M. Donadelli, B. Dong, X. Dong, Z. Dong, G. W. Dorn Ii, V. Dotsch, H. Dou, J. Dou, M. Dowaidar, S. Dridi, L. Drucker, A. Du, C. Du, G. Du, H.N. Du, L.L. Du, A. du Toit, S.B. Duan, X. Duan, S.P. Duarte, A. Dubrovska, E.A. Dunlop, N. Dupont, R.V. Duran, B.S. Dwarakanath, S. A. Dyshlovoy, D. Ebrahimi-Fakhari, L. Eckhart, C.L. Edelstein, T. Efferth, E. Eftekharpour, L. Eichinger, N. Eid, T. Eisenberg, N.T. Eissa, S. Eissa, M. Ejarque, A. El Andaloussi, N. El-Hage, S. El-Naggar, A.M. Eleuteri, E.S. El-Shafey, M. Elgendy, A.G. Eliopoulos, M.M. Elizalde, P.M. Elks, H.P. Elsasser, E. S. Elsherbiny, B.M. Emerling, N.C.T. Emre, C.H. Eng, N. Engedal, A.M. Engelbrecht, A.S.T. Engelsen, J.M. Enserink, R. Escalante, A. Esclatine, M. Escobar-Henriques, E. L. Eskelinen, L. Espert, M.O. Eusebio, G. Fabrias, C. Fabrizi, A. Facchiano, F. Facchiano, B. Fadeel, C. Fader, A.C. Faesen, W.D. Fairlie, A. Falco, B. H. Falkenburger, D. Fan, J. Fan, Y. Fan, E.F. Fang, Y. Fang, Y. Fang, M. Fanto, T. Farfel-Becker, M. Faure, G. Fazeli, A.O. Fedele, A.M. Feldman, D. Feng, J. Feng, L. Feng, Y. Feng, Y. Feng, W. Feng, T. Fenz Araujo, T.A. Ferguson, A.F. Fernandez, J.C. Fernandez-Checa, S. Fernandez-Veledo, A.R. Fernie, A.W. Ferrante Jr., A. Ferraresi, M.F. Ferrari, J.C.B. Ferreira, S. Ferro-Novick, A. Figueras, R. Filadi, N. Filigheddu, E. Filippi-Chiela, G. Filomeni, G.M. Fimia, V. Fineschi, F. Finetti, S. Finkbeiner, E.A. Fisher, P.B. Fisher, F. Flamigni, S.J. Fliesler, T.H. Flo, I. Florance, O. Florey, T. Florio, E. Fodor, C. Follo, E.A. Fon, A. Forlino, F. Fornai, P. Fortini, A. Fracassi, A. Fraldi, B. Franco, R. Franco, F. Franconi, L.B. Frankel, S. L. Friedman, L.F. Frohlich, G. Fruhbeck, J.M. Fuentes, Y. Fujiki, N. Fujita, Y. Fujiwara, M. Fukuda, S. Fulda, L. Furic, N. Furuya, C. Fusco, M.U. Gack, L. Gaffke, S. Galadari, A. Galasso, M.F. Galindo, S. Gallolu Kankanamalage, L. Galluzzi, V. Galy, N. Gammoh, B. Gan, I.G. Ganley, F. Gao, H. Gao, M. Gao, P. Gao, S.J. Gao, W. Gao, X. Gao, A. Garcera, M.N. Garcia, V.E. Garcia, F. Garcia-Del Portillo, V. Garcia-Escudero, A. Garcia-Garcia, M. Garcia-Macia, D. Garcia-Moreno, C. Garcia-Ruiz, P. Garcia-Sanz, A.D. Garg, R. Gargini, T. Garofalo, R. F. Garry, N.C. Gassen, D. Gatica, L. Ge, W. Ge, R. Geiss-Friedlander, C. Gelfi, P. Genschik, I.E. Gentle, V. Gerbino, C. Gerhardt, K. Germain, M. Germain, D. A. Gewirtz, E. Ghasemipour Afshar, S. Ghavami, A. Ghigo, M. Ghosh, G. Giamas, C. Giampietri, A. Giatromanolaki, G.E. Gibson, S.B. Gibson, V. Ginet, E. Giniger, C. Giorgi, H. Girao, S.E. Girardin, M. Giridharan, S. Giuliano, C. Giulivi, S. Giuriato, J. Giustiniani, A. Gluschko, V. Goder, A. Goginashvili, J. Golab, D.C. Goldstone, A. Golebiewska, L.R. Gomes, R. Gomez, R. Gomez-Sanchez, M.C. Gomez-Puerto, R. Gomez-Sintes, Q. Gong, F.M. Goni, J. Gonzalez-Gallego, T. Gonzalez-Hernandez, R.A. Gonzalez-Polo, J.A. Gonzalez-Reyes, P. Gonzalez-Rodriguez, I.S. Goping, M. S. Gorbatyuk, N.V. Gorbunov, K. Gorgulu, R.M. Gorojod, S.M. Gorski, S. Goruppi, C. Gotor, R.A. Gottlieb, I. Gozes, D. Gozuacik, M. Graef, M.H. Graler, V. Granatiero, D. Grasso, J.P. Gray, D.R. Green, A. Greenhough, S.L. Gregory, E.F. Griffin, M. W. Grinstaff, F. Gros, C. Grose, A.S. Gross, F. Gruber, P. Grumati, T. Grune, X. Gu, J. L. Guan, C.M. Guardia, K. Guda, F. Guerra, C. Guerri, P. Guha, C. Guillen, S. Gujar, A. Gukovskaya, I. Gukovsky, J. Gunst, A. Gunther, A.R. Guntur, C. Guo, C. Guo, H. Guo, L.W. Guo, M. Guo, P. Gupta, S.K. Gupta, S. Gupta, V.B. Gupta, V. Gupta, A. B. Gustafsson, D.D. Gutterman, B.R. H, A. Haapasalo, J.E. Haber, A. Hac, S. Hadano, A.J. Hafren, M. Haidar, B.S. Hall, G. Hallden, A. Hamacher-Brady, A. Hamann, M. Hamasaki, W. Han, M. Hansen, P.I. Hanson, Z. Hao, M. Harada, L. Harhaji-Trajkovic, N. Hariharan, N. Haroon, J. Harris, T. Hasegawa, N. Hasima Nagoor, J.A. Haspel, V. Haucke, W.D. Hawkins, B.A. Hay, C.M. Haynes, S. B. Hayrabedyan, T.S. Hays, C. He, Q. He, R.R. He, Y.W. He, Y.Y. He, Y. Heakal, A. M. Heberle, J.F. Hejtmancik, G.V. Helgason, V. Henkel, M. Herb, A. Hergovich, A. Herman-Antosiewicz, A. Hernandez, C. Hernandez, S. Hernandez-Diaz, V. Hernandez-Gea, A. Herpin, J. Herreros, J.H. Hervas, D. Hesselson, C. Hetz, V. T. Heussler, Y. Higuchi, S. Hilfiker, J.A. Hill, W.S. Hlavacek, E.A. Ho, I.H.T. Ho, P. W. Ho, S.L. Ho, W.Y. Ho, G.A. Hobbs, M. Hochstrasser, P.H.M. Hoet, D. Hofius, P. Hofman, A. Hohn, C.I. Holmberg, J.R. Hombrebueno, C.H. Yi-Ren Hong, L. V. Hooper, T. Hoppe, R. Horos, Y. Hoshida, I.L. Hsin, H.Y. Hsu, B. Hu, D. Hu, L. F. Hu, M.C. Hu, R. Hu, W. Hu, Y.C. Hu, Z.W. Hu, F. Hua, J. Hua, Y. Hua, C. Huan, C. Huang, C. Huang, C. Huang, C. Huang, H. Huang, K. Huang, M.L.H. Huang, R. Huang, S. Huang, T. Huang, X. Huang, Y.J. Huang, T.B. Huber, V. Hubert, C. A. Hubner, S.M. Hughes, W.E. Hughes, M. Humbert, G. Hummer, J.H. Hurley, S. Hussain, S. Hussain, P.J. Hussey, M. Hutabarat, H.Y. Hwang, S. Hwang, A. Ieni, F. Ikeda, Y. Imagawa, Y. Imai, C. Imbriano, M. Imoto, D.M. Inman, K. Inoki, J. Iovanna, R.V. Iozzo, G. Ippolito, J.E. Irazoqui, P. Iribarren, M. Ishaq, M. Ishikawa, N. Ishimwe, C. Isidoro, N. Ismail, S. Issazadeh-Navikas, E. Itakura, D. Ito, D. Ivankovic, S. Ivanova, A.K.V. Iyer, J.M. Izquierdo, M. Izumi, M. Jaattela, M.S. Jabir, W.T. Jackson, N. Jacobo-Herrera, A.C. Jacomin, E. Jacquin, P. Jadiya, H. Jaeschke, C. Jagannath, A.J. Jakobi, J. Jakobsson, B. Janji, P. Jansen-Durr, P. J. Jansson, J. Jantsch, S. Januszewski, A. Jassey, S. Jean, H. Jeltsch-David, P. Jendelova, A. Jenny, T.E. Jensen, N. Jessen, J.L. Jewell, J. Ji, L. Jia, R. Jia, L. Jiang, Q. Jiang, R. Jiang, T. Jiang, X. Jiang, Y. Jiang, M. Jimenez-Sanchez, E. J. Jin, F. Jin, H. Jin, L. Jin, L. Jin, M. Jin, S. Jin, E.K. Jo, C. Joffre, T. Johansen, G.V. W. Johnson, S.A. Johnston, E. Jokitalo, M.K. Jolly, L.A.B. Joosten, J. Jordan, B. Joseph, D. Ju, J.S. Ju, J. Ju, E. Juarez, D. Judith, G. Juhasz, Y. Jun, C.H. Jung, S. C. Jung, Y.K. Jung, H. Jungbluth, J. Jungverdorben, S. Just, K. Kaarniranta, A. Kaasik, T. Kabuta, D. Kaganovich, A. Kahana, R. Kain, S. Kajimura, M. Kalamvoki, M. Kalia, D.S. Kalinowski, N. Kaludercic, I. Kalvari, J. Kaminska, V. O. Kaminskyy, H. Kanamori, K. Kanasaki, C. Kang, R. Kang, S.S. Kang, S. Kaniyappan, T. Kanki, T.D. Kanneganti, A.G. Kanthasamy, A. Kanthasamy, M. Kantorow, O. Kapuy, M.V. Karamouzis, M.R. Karim, P. Karmakar, R.G. Katare, M. Kato, S.H.E. Kaufmann, A. Kauppinen, G.P. Kaushal, S. Kaushik, K. Kawasaki, K. Kazan, P.Y. Ke, D.J. Keating, U. Keber, J.H. Kehrl, K.E. Keller, C.W. Keller, J. K. Kemper, C.M. Kenific, O. Kepp, S. Kermorgant, A. Kern, R. Ketteler, T.G. Keulers, B. Khalfin, H. Khalil, B. Khambu, S.Y. Khan, V.K.M. Khandelwal, R. Khandia, W. Kho, N.V. Khobrekar, S. Khuansuwan, M. Khundadze, S.A. Killackey, D. Kim, D. R. Kim, D.H. Kim, D.E. Kim, E.Y. Kim, E.K. Kim, H.R. Kim, H.S. Kim, K. Hyung-Ryong, J.H. Kim, J.K. Kim, J.H. Kim, J. Kim, J.H. Kim, K.I. Kim, P.K. Kim, S.J. Kim, S.R. Kimball, A. Kimchi, A.C. Kimmelman, T. Kimura, M.A. King, K.J. Kinghorn, C. G. Kinsey, V. Kirkin, L.A. Kirshenbaum, S.L. Kiselev, S. Kishi, K. Kitamoto, Y. Kitaoka, K. Kitazato, R.N. Kitsis, J.T. Kittler, O. Kjaerulff, P.S. Klein, T. Klopstock, J. Klucken, H. Knaevelsrud, R.L. Knorr, B.C.B. Ko, F. Ko, J.L. Ko, H. Kobayashi, S. Kobayashi, I. Koch, J.C. Koch, U. Koenig, D. Kogel, Y.H. Koh, M. Koike, S.D. Kohlwein, N.M. Kocaturk, M. Komatsu, J. Konig, T. Kono, B.T. Kopp, T. Korcsmaros, G. Korkmaz, V.I. Korolchuk, M.S. Korsnes, A. Koskela, J. Kota, Y. Kotake, M.L. Kotler, Y. Kou, M.I. Koukourakis, E. Koustas, A.L. Kovacs, T. Kovacs, D. Koya, T. Kozako, C. Kraft, D. Krainc, H. Kramer, A. D. Krasnodembskaya, C. Kretz-Remy, G. Kroemer, N.T. Ktistakis, K. Kuchitsu, S. Kuenen, L. Kuerschner, T. Kukar, A. Kumar, A. Kumar, D. Kumar, D. Kumar, S. Kumar, S. Kume, C. Kumsta, C.N. Kundu, M. Kundu, A.B. Kunnumakkara, L. Kurgan, T.G. Kutateladze, O. Kutlu, S. Kwak, H.J. Kwon, T.K. Kwon, Y.T. Kwon, I. Kyrmizi, A. La Spada, P. Labonte, S. Ladoire, I. Laface, F. Lafont, D.C. Lagace, V. Lahiri, Z. Lai, A.S. Laird, A. Lakkaraju, T. Lamark, S.H. Lan, A. Landajuela, D.J. R. Lane, J.D. Lane, C.H. Lang, C. Lange, U. Langel, R. Langer, P. Lapaquette, J. Laporte, N.F. LaRusso, I. Lastres-Becker, W.C.Y. Lau, G.W. Laurie, S. Lavandero, B.Y.K. Law, H.K. Law, R. Layfield, W. Le, H. Le Stunff, A.Y. Leary, J.J. Lebrun, L.Y. W. Leck, J.P. Leduc-Gaudet, C. Lee, C.P. Lee, D.H. Lee, E.B. Lee, E.F. Lee, G.M. Lee, H.J. Lee, H.K. Lee, J.M. Lee, J.S. Lee, J.A. Lee, J.Y. Lee, J.H. Lee, M. Lee, M.G. Lee, M.J. Lee, M.S. Lee, S.Y. Lee, S.J. Lee, S.Y. Lee, S.B. Lee, W.H. Lee, Y.R. Lee, Y. H. Lee, Y. Lee, C. Lefebvre, R. Legouis, Y.L. Lei, Y. Lei, S. Leikin, G. Leitinger, L. Lemus, S. Leng, O. Lenoir, G. Lenz, H.J. Lenz, P. Lenzi, Y. Leon, A.M. Leopoldino, C. Leschczyk, S. Leskela, E. Letellier, C.T. Leung, P.S. Leung, J.S. Leventhal, B. Levine, P.A. Lewis, K. Ley, B. Li, D.Q. Li, J. Li, J. Li, J. Li, K. Li, L. Li, M. Li, M. Li, M. Li, M. Li, P.L. Li, M.Q. Li, Q. Li, S. Li, T. Li, W. Li, W. Li, X. Li, Y.P. Li, Y. Li, Z. Li, Z. Li, Z. Li, J. Lian, C. Liang, Q. Liang, W. Liang, Y. Liang, G. Liao, L. Liao, M. Liao, Y.F. Liao, M. Librizzi, P.P.Y. Lie, M.A. Lilly, H.J. Lim, T.R.R. Lima, F. Limana, C. Lin, C.W. Lin, D.S. Lin, F.C. Lin, J.D. Lin, K.M. Lin, K.H. Lin, L.T. Lin, P.H. Lin, Q. Lin, S. Lin, S.J. Lin, W. Lin, X. Lin, Y.X. Lin, Y.S. Lin, R. Linden, P. Lindner, S.C. Ling, P. Lingor, A.K. Linnemann, Y.C. Liou, M.M. Lipinski, S. Lipovsek, V.A. Lira, N. Lisiak, P.B. Liton, C. Liu, C.H. Liu, C.F. Liu, C.H. Liu,

F. Liu, H. Liu, H.S. Liu, H.F. Liu, H. Liu, J. Liu, J. Liu, J. Liu, L. Liu, L. Liu, M. Liu, Q. Liu, W. Liu, W. Liu, X.H. Liu, X. Liu, X. Liu, X. Liu, X. Liu, Y. Liu, Y. Liu, Y. Liu, Y. Liu, Y. Liu, J.A. Livingston, G. Lizard, J.M. Lizcano, S. Ljubojevic-Holzer, L. L. Me, D. Llobet-Navas, A. Llorente, C.H. Lo, D. Lobato-Marquez, Q. Long, Y. C. Long, B. Loos, J.A. Loos, M.G. Lopez, G. Lopez-Domenech, J.A. Lopez-Guerrero, A.T. Lopez-Jimenez, O. Lopez-Perez, I. Lopez-Valero, M.J. Lorenowicz, M. Lorente, P. Lorincz, L. Lossi, S. Lotersztajn, P.E. Lovat, J.F. Lovell, A. Lovy, P. Low, G. Lu, H. Lu, J.H. Lu, J.J. Lu, M. Lu, S. Lu, A. Luciani, J.M. Lucocq, P. Ludovico, M. A. Luftig, M. Luhr, D. Luis-Ravelo, J.J. Lum, L. Luna-Dulcey, A.H. Lund, V.K. Lund, J.D. Lunemann, P. Luningschror, H. Luo, R. Luo, S. Luo, Z. Luo, C. Luparello, B. Luscher, L. Luu, A. Lyakhovich, K.G. Lyamzaev, A.H. Lystad, L. Lytvynchuk, A. C. Ma, C. Ma, M. Ma, N.F. Ma, Q.H. Ma, X. Ma, Y. Ma, Z. Ma, O.A. MacDougald, F. Macian, G.C. MacIntosh, J.P. MacKeigan, K.F. Macleod, S. Maday, F. Madeo, M. Madesh, T. Madl, J. Madrigal-Matute, A. Maeda, Y. Maejima, M. Magarinos, P. Mahavadi, E. Maiani, K. Maiese, P. Maiti, M.C. Maiuri, B. Majello, M.B. Major, E. Makareeva, F. Malik, K. Mallilankaraman, W. Malorni, A. Maloyan, N. Mammadova, G.C.W. Man, F. Manai, J.D. Mancias, E.M. Mandelkow, M. A. Mandell, A.A. Manfredi, M.H. Manjili, R. Manjithaya, P. Manque, B. B. Manshian, R. Manzano, C. Manzoni, K. Mao, C. Marchese, S. Marchetti, A. M. Marconi, F. Marcucci, S. Mardente, O.A. Mareninova, M. Margeta, M. Mari, S. Marinelli, O. Marinelli, G. Marino, S. Mariotto, R.S. Marshall, M.R. Marten, S. Martens, A.P.J. Martin, K.R. Martin, S. Martin, S. Martin, A. Martin-Segura, M. A. Martin-Acebes, I. Martin-Burriel, M. Martin-Rincon, P. Martin-Sanz, J. A. Martina, W. Martinet, A. Martinez, A. Martinez, J. Martinez, M. Martinez Velazquez, N. Martinez-Lopez, M. Martinez-Vicente, D.O. Martins, J.O. Martins, W. K. Martins, T. Martins-Marques, E. Marzetti, S. Masaldan, C. Masclaux-Daubresse, D.G. Mashek, V. Massa, L. Massieu, G.R. Masson, L. Masuelli, A.I. Masyuk, T. V. Masyuk, P. Matarrese, A. Matheu, S. Matoba, S. Matsuzaki, P. Mattar, A. Matte, D. Mattoscio, J.L. Mauriz, M. Mauthe, C. Mauvezin, E. Maverakis, P. Maycotte, J. Mayer, G. Mazzoccoli, C. Mazzoni, J.R. Mazzulli, N. McCarty, C. McDonald, M. R. McGill, S.L. McKenna, B. McLaughlin, F. McLoughlin, M.A. McNiven, T. G. McWilliams, F. Mechta-Grigoriou, T.C. Medeiros, D.L. Medina, L.A. Megeney, K. Megyeri, M. Mehrpour, J.L. Mehta, A.J. Meijer, A.H. Meijer, J. Mejlvang, A. Melendez, A. Melk, G. Memisoglu, A.F. Mendes, D. Meng, F. Meng, T. Meng, R. Menna-Barreto, M.B. Menon, C. Mercer, A.E. Mercier, J.L. Mergny, A. Merighi, S.D. Merkley, G. Merla, V. Meske, A.C. Mestre, S.P. Metur, C. Meyer, H. Meyer, W. Mi, J. Mialet-Perez, J. Miao, L. Micale, Y. Miki, E. Milan, M. Milczarek, D. L. Miller, S.I. Miller, S. Miller, S.W. Millward, I. Milosevic, E.A. Minina, H. Mirzaei, H.R. Mirzaei, M. Mirzaei, A. Mishra, N. Mishra, P.K. Mishra, M. Misirkic Marjanovic, R. Misasi, A. Misra, G. Misso, C. Mitchell, G. Mitou, T. Miura, S. Miyamoto, M. Miyazaki, M. Miyazaki, T. Miyazaki, K. Miyazawa, N. Mizushima, T.H. Mogensen, B. Mograbi, R. Mohammadinejad, Y. Mohamud, A. Mohanty, S. Mohapatra, T. Mohlmann, A. Mohmmed, A. Moles, K.H. Moley, M. Molinari, V. Mollace, A.B. Moller, B. Mollereau, F. Mollinedo, C. Montagna, M.J. Monteiro, A. Montella, L.R. Montes, B. Montico, V.K. Mony, G. Monzio Compagnoni, M. N. Moore, M.A. Moosavi, A.L. Mora, M. Mora, D. Morales-Alamo, R. Moratalla, P. I. Moreira, E. Morelli, S. Moreno, D. Moreno-Blas, V. Moresi, B. Morga, A. H. Morgan, F. Morin, H. Morishita, O.L. Moritz, M. Moriyama, Y. Moriyasu, M. Morleo, E. Morselli, J.F. Moruno-Manchon, J. Moscat, S. Mostowy, E. Motori, A. F. Moura, N. Moustaid-Moussa, M. Mrakovcic, G. Mucino-Hernandez, A. Mukherjee, S. Mukhopadhyay, J.M. Mulcahy Levy, V. Mulero, S. Muller, C. Munch, A. Munjal, P. Munoz-Canoves, T. Munoz-Galdeano, C. Munz, T. Murakawa, C. Muratori, B.M. Murphy, J.P. Murphy, A. Murthy, T.T. Myohanen, I.U. Mysorekar, J. Mytych, S.M. Nabavi, M. Nabissi, P. Nagy, J. Nah, A. Nahimana, I. Nakagawa, K. Nakamura, H. Nakatogawa, S.S. Nandi, M. Nanjundan, M. Nanni, G. Napolitano, R. Nardacci, M. Narita, M. Nassif, I. Nathan, M. Natsumeda, R. J. Naude, C. Naumann, O. Naveiras, F. Navid, S.T. Nawrocki, T.Y. Nazarko, F. Nazio, F. Negoita, T. Neill, A.L. Neisch, L.M. Neri, M.G. Netea, P. Neubert, T. P. Neufeld, D. Neumann, A. Neutzner, P.T. Newton, P.A. Ney, I.P. Nezis, C.C.W. Ng, T.B. Ng, H.T.T. Nguyen, L.T. Nguyen, H.M. Ni, C. Ni Cheallaigh, Z. Ni, M. C. Nicolao, F. Nicoli, M. Nieto-Diaz, P. Nilsson, S. Ning, R. Niranjan, H. Nishimune, M. Niso-Santano, R.A. Nixon, A. Nobili, C. Nobrega, T. Noda, U. Nogueira-Recalde, T.M. Nolan, I. Nombela, I. Novak, B. Novoa, T. Nozawa, N. Nukina, C. Nussbaum-Krammer, J. Nylandsted, T.R. O'Donovan, S.M. O'Leary, E.J. O'Rourke, M. P. O'Sullivan, T.E. O'Sullivan, S. Oddo, I. Oehme, M. Ogawa, E. Ogier-Denis, M. H. Ogmundsdottir, B. Ogretmen, G.T. Oh, S.H. Oh, Y.J. Oh, T. Ohama, Y. Ohashi, M. Ohmuraya, V. Oikonomou, R. Ojha, K. Okamoto, H. Okazawa, M. Oku, S. Olivan, J.M.A. Oliveira, M. Ollmann, J.A. Olzmann, S. Omari, M.B. Omary, G. Onal, M. Ondrej, S.B. Ong, S.G. Ong, A. Onnis, J.A. Orellana, S. Orellana-Munoz, M.D.M. Ortega-Villaizan, X.R. Ortiz-Gonzalez, E. Ortona, H.D. Osiewacz, A. K. Osman, R. Osta, M.S. Otegui, K. Otsu, C. Ott, L. Ottobrini, J.J. Ou, T.F. Outeiro, I. Oynebraten, M. Ozturk, G. Pages, S. Pahari, M. Pajares, U.B. Pajvani, R. Pal, S. Paladino, N. Pallet, M. Palmieri, G. Palmisano, C. Palumbo, F. Pampaloni, L. Pan, Q. Pan, W. Pan, X. Pan, G. Panasyuk, R. Pandey, U.B. Pandey, V. Pandya, F. Paneni, S.Y. Pang, E. Panzarini, D.L. Papademetrio, E. Papaleo, D. Papinski, D. Papp, E. C. Park, H.T. Park, J.M. Park, J.I. Park, J.T. Park, J. Park, S.C. Park, S.Y. Park, A. H. Parola, J.B. Parys, A. Pasquier, B. Pasquier, J.F. Passos, N. Pastore, H.H. Patel, D. Patschan, S. Pattingre, G. Pedraza-Alva, J. Pedraza-Chaverri, Z. Pedrozo, G. Pei, J. Pei, H. Peled-Zehavi, J.M. Pellegrini, J. Pelletier, M.A. Penalva, D. Peng, Y. Peng, F. Penna, M. Pennuto, F. Pentimalli, C.M. Pereira, G.J.S. Pereira, L.C. Pereira, L. Pereira de Almeida, N.D. Perera, A. Perez-Lara, A.B. Perez-Oliva, M.E. Perez-Perez, P. Periyasamy, A. Perl, C. Perrotta, I. Perrotta, R.G. Pestell, M. Petersen, I. Petrache, G. Petrovski, T. Pfirrmann, A.S. Pfister, J.A. Philips, H. Pi, A. Picca, A. M. Pickrell, S. Picot, G.M. Pierantoni, M. Pierdominici, P. Pierre, V. Pierrefite-Carle, K. Pierzynowska, F. Pietrocola, M. Pietruczuk, C. Pignata, F.X. Pimentel-Muinos, M. Pinar, R.O. Pinheiro, R. Pinkas-Kramarski, P. Pinton, K. Pircs, S. Piya, P. Pizzo, T.S. Plantinga, H.W. Platta, A. Plaza-Zabala, M. Plomann, E.Y. Plotnikov, H. Plun-Favreau, R. Pluta, R. Pocock, S. Poggeler, C. Pohl, M. Poirot, A. Poletti, M. Ponpuak, H. Popelka, B. Popova, H. Porta, S. Porte Alcon, E. Portilla-Fernandez, M. Post, M.B. Potts, J. Poulton, T. Powers, V. Prahlad, T.K. Prajsnar, D. Pratico, R. Prencipe, M. Priault, T. Proikas-Cezanne, V.J. Promponas, C.G. Proud, R. Puertollano, L. Puglielli, T. Pulinilkunnil, D. Puri, R. Puri, J. Puyal, X. Qi, Y. Qi, W. Qian, L. Qiang, Y. Qiu, J. Quadrilatero, J. Quarleri, N. Raben, H. Rabinowich, D. Ragona, M.J. Ragusa, N. Rahimi, M. Rahmati, V. Raia, N. Raimundo, N. S. Rajasekaran, S. Ramachandra Rao, A. Rami, I. Ramirez-Pardo, D.B. Ramsden, F. Randow, P.N. Rangarajan, D. Ranieri, H. Rao, L. Rao, R. Rao, S. Rathore, J. A. Ratnayaka, E.A. Ratovitski, P. Ravanan, G. Ravegnini, S.K. Ray, B. Razani, V. Rebecca, F. Reggiori, A. Regnier-Vigouroux, A.S. Reichert, D. Reigada, J. H. Reiling, T. Rein, S. Reipert, R.S. Rekha, H. Ren, J. Ren, W. Ren, T. Renault, G. Renga, K. Reue, K. Rewitz, B. Ribeiro de Andrade Ramos, S.A. Riazuddin, T. M. Ribeiro-Rodrigues, J.E. Ricci, R. Ricci, V. Riccio, D.R. Richardson, Y. Rikihisa, M.V. Risbud, R.M. Risueno, K. Ritis, S. Rizza, R. Rizzuto, H.C. Roberts, L. D. Roberts, K.J. Robinson, M.C. Roccheri, S. Rocchi, G.G. Rodney, T. Rodrigues, V. R. Rodrigues Silva, A. Rodriguez, R. Rodriguez-Barrueco, N. Rodriguez-Henche, H. Rodriguez-Rocha, J. Roelofs, R.S. Rogers, V.V. Rogov, A.I. Rojo, K. Rolka, V. Romanello, L. Romani, A. Romano, P.S. Romano, D. Romeo-Guitart, L. C. Romero, M. Romero, J.C. Roney, C. Rongo, S. Roperto, M.T. Rosenfeldt, P. Rosenstiel, A.G. Rosenwald, K.A. Roth, L. Roth, S. Roth, K.M.A. Rouschop, B. D. Roussel, S. Roux, P. Rovere-Querini, A. Roy, A. Rozieres, D. Ruano, D. C. Rubinsztein, M.P. Rubtsova, K. Ruckdeschel, C. Ruckenstuhl, E. Rudolf, R. Rudolf, A. Ruggieri, A.A. Ruparelia, P. Rusmini, R.R. Russell, G.L. Russo, M. Russo, R. Russo, O.O. Ryabaya, K.M. Ryan, K.Y. Ryu, M. Sabater-Arcis, U. Sachdev, M. Sacher, C. Sachse, A. Sadhu, J. Sadoshima, N. Safren, P. Saftig, A. P. Sagona, G. Sahay, A. Sahebkar, M. Sahin, O. Sahin, S. Sahni, N. Saito, S. Saito, T. Saito, R. Sakai, Y. Sakai, J.I. Sakamaki, K. Saksela, G. Salazar, A. Salazar-Degracia, G.H. Salekdeh, A.K. Saluja, B. Sampaio-Marques, M.C. Sanchez, J. A. Sanchez-Alcazar, V. Sanchez-Vera, V. Sancho-Shimizu, J.T. Sanderson, M. Sandri, S. Santaguida, L. Santambrogio, M.M. Santana, G. Santoni, A. Sanz, P. Sanz, S. Saran, M. Sardiello, T.J. Sargeant, A. Sarin, C. Sarkar, S. Sarkar, M. R. Sarrias, S. Sarkar, D.T. Sarmah, J. Sarparanta, A. Sathyanarayan, R. Sathyanarayanan, K.M. Scaglione, F. Scatozza, L. Schaefer, Z.T. Schafer, U. E. Schaible, A.H.V. Schapira, M. Scharl, H.M. Schatzl, C.H. Schein, W. Scheper, D. Scheuring, M.V. Schiaffino, M. Schiappacassi, R. Schindl, U. Schlattner, O. Schmidt, R. Schmitt, S.D. Schmidt, I. Schmitz, E. Schmukler, A. Schneider, B. E. Schneider, R. Schober, A.C. Schoijet, M.B. Schott, M. Schramm, B. Schroder, K. Schuh, C. Schuller, R.J. Schulze, L. Schurmanns, J.C. Schwamborn, M. Schwarten, F. Scialo, S. Sciarretta, M.J. Scott, K.W. Scotto, A.I. Scovassi, A. Scrima, A. Scrivo, D. Sebastian, S. Sebti, S. Sedej, L. Segatori, N. Segev, P. O. Seglen, I. Seiliez, E. Seki, S.B. Selleck, F.W. Sellke, J.T. Selsby, M. Sendtner, S. Senturk, E. Seranova, C. Sergi, R. Serra-Moreno, H. Sesaki, C. Settembre, S.R. G. Setty, G. Sgarbi, O. Sha, J.J. Shacka, J.A. Shah, D. Shang, C. Shao, F. Shao, S. Sharbati, L.M. Sharkey, D. Sharma, G. Sharma, K. Sharma, P. Sharma, S. Sharma, H.M. Shen, H. Shen, J. Shen, M. Shen, W. Shen, Z. Shen, R. Sheng, Z. Sheng, Z. H. Sheng, J. Shi, X. Shi, Y.H. Shi, K. Shiba-Fukushima, J.J. Shieh, Y. Shimada, S. Shimizu, M. Shimozawa, T. Shintani, C.J. Shoemaker, S. Shojaei, I. Shoji, B. V. Shravage, V. Shridhar, C.W. Shu, H.B. Shu, K. Shui, A.K. Shukla, T.E. Shutt, V. Sica, A. Siddiqui, A. Sierra, V. Sierra-Torre, S. Signorelli, P. Sil, B.J.A. Silva, J. D. Silva, E. Silva-Pavez, S. Silvente-Poirot, R.E. Simmonds, A.K. Simon, H. U. Simon, M. Simons, A. Singh, L.P. Singh, R. Singh, S.V. Singh, S.K. Singh, S. B. Singh, S. Singh, S.P. Singh, D. Sinha, R.A. Sinha, S. Sinha, A. Sirko, K. Sirohi, E. L. Sivridis, P. Skendros, A. Skirycz, I. Slaninova, S.S. Smaili, A. Smertenko, M. D. Smith, S.J. Soenen, E.J. Sohn, S.P.M. Sok, G. Solaini, T. Soldati, S. A. Soleimanpour, R.M. Soler, A. Solovchenko, J.A. Somarelli, A. Sonawane, F. Song, H.K. Song, J.X. Song, K. Song, Z. Song, L.R. Soria, M. Sorice, A.A. Soukas, S.F. Soukup, D. Sousa, N. Sousa, P.A. Spagnuolo, S.A. Spector, M.M. Srinivas Bharath, D. St Clair, V. Stagni, L. Staiano, C.A. Stalnecker, M.V. Stankov, P. B. Stathopulos, K. Stefan, S.M. Stefan, L. Stefanis, J.S. Steffan, A. Steinkasserer, H. Stenmark, J. Sterneckert, C. Stevens, V. Stoka, S. Storch, B. Stork, F. Strappazzon, A.M. Strohecker, D.G. Stupack, H. Su, L.Y. Su, L. Su, A.M. Suarez-Fontes, C.S. Subauste, S. Subbian, P.V. Subirada, G. Sudhandiran, C.M. Sue, X. Sui, C. Summers, G. Sun, J. Sun, K. Sun, M.X. Sun, Q. Sun, Y. Sun, Z. Sun, K.K. S. Sunahara, E. Sundberg, K. Susztak, P. Sutovsky, H. Suzuki, G. Sweeney, J. D. Symons, S.C.W. Sze, N.J. Szewczyk, A. Tabecka-Lonczynska, C. Tabolacci, F. Tacke, H. Taegtmeyer, M. Tafani, M. Tagaya, H. Tai, S.W.G. Tait, Y. Takahashi, S. Takats, P. Talwar, C. Tam, S.Y. Tam, D. Tampellini, A. Tamura, C.T. Tan, E. K. Tan, Y.Q. Tan, M. Tanaka, M. Tanaka, D. Tang, J. Tang, T.S. Tang, I. Tanida, Z. Tao, M. Taouis, L. Tatenhorst, N. Tavernarakis, A. Taylor, G.A. Taylor, J. M. Taylor, E. Tchetina, A.R. Tee, I. Tegeder, D. Teis, N. Teixeira, F. Teixeira-Clerc, K.A. Tekirdag, T. Tencomnao, S. Tenreiro, A.V. Tepikin, P.S. Testillano, G. Tettamanti, P.L. Tharaux, K. Thedieck, A.A. Thekkinghat, S. Thellung, J. W. Thinwa, V.P. Thirumalaikumar, S.M. Thomas, P.G. Thomes, A. Thorburn, L. Thukral, T. Thum, M. Thumm, L. Tian, A. Tichy, A. Till, V. Timmerman, V. I. Titorenko, S.V. Todi, K. Todorova, J.M. Toivonen, L. Tomaipitinca, D. Tomar, C. Tomas-Zapico, S. Tomic, B.C. Tong, C. Tong, X. Tong, S.A. Tooze, M. L. Torgersen, S. Torii, L. Torres-Lopez, A. Torriglia, C.G. Towers, R. Towns, S. Toyokuni, V. Trajkovic, D. Tramontano, Q.G. Tran, L.H. Travassos, C.B. Trelford, S. Tremel, I.P. Trougakos, B.P. Tsao, M.P. Tschan, H.F. Tse, T.F. Tse, H. Tsugawa, A.S. Tsvetkov, D.A. Tumbarello, Y. Tumtas, M.J. Tunon, S. Turcotte, B. Turk, V. Turk, B.J. Turner, R.I. Tuxworth, J.K. Tyler, E.V. Tyutereva, Y. Uchiyama, A. Ugun-Klusek, H.H. Uhlig, M. Ulamek-Koziol, I.V. Ulasov, M. Umekawa, C. Ungermann, R. Unno, S. Urbe, E. Uribe-Carretero, S. Ustun, V.N. Uversky, T. Vaccari, M.I. Vaccaro, B.F. Vahsen, H. Vakifahmetoglu-Norberg, R. Valdor, M.

J. Valente, A. Valko, R.B. Vallee, A.M. Valverde, G. Van den Berghe, S. van der Veen, L. Van Kaer, J. van Loosdregt, S.J.L. van Wijk, W. Vandenberghe, I. Vanhorebeek, M.A. Vannier-Santos, N. Vannini, M.C. Vanrell, C. Vantaggiato, G. Varano, I. Varela-Nieto, M. Varga, M.H. Vasconcelos, S. Vats, D.G. Vavvas, I. Vega-Naredo, S. Vega-Rubin-de-Celis, G. Velasco, A.P. Velazquez, T. Vellai, E. Vellenga, F. Velotti, M. Verdier, P. Verginis, I. Vergne, P. Verkade, M. Verma, P. Verstreken, T. Vervliet, J. Vervoorts, A.T. Vessoni, V.M. Victor, M. Vidal, C. Vidoni, O.V. Vieira, R.D. Vierstra, S. Vigano, H. Vihinen, V. Vijayan, M. Vila, M. Vilar, J.M. Villalba, A. Villalobo, B. Villarejo-Zori, F. Villarroya, J. Villarroya, O. Vincent, C. Vindis, C. Viret, M.T. Viscomi, D. Visnjic, I. Vitale, D.J. Vocadlo, O. V. Voitsekhovskaja, C. Volonte, M. Volta, M. Vomero, C. Von Haefen, M.A. Vooijs, W. Voos, L. Vucicevic, R. Wade-Martins, S. Waguri, K.A. Waite, S. Wakatsuki, D. W. Walker, M.J. Walker, S.A. Walker, J. Walter, F.G. Wandosell, B. Wang, C. Y. Wang, C. Wang, C. Wang, C.Y. Wang, D. Wang, F. Wang, F. Wang, F. Wang, G. Wang, H. Wang, H. Wang, H.G. Wang, J. Wang, J. Wang, J. Wang, J. Wang, K. Wang, L. Wang, L. Wang, M.H. Wang, M. Wang, N. Wang, P. Wang, P. Wang, P. Wang, P. Wang, Q.J. Wang, Q. Wang, Q.K. Wang, Q.A. Wang, W.T. Wang, W. Wang, X. Wang, X. Wang, Y. Wang, Y. Wang, Y. Wang, Y.Y. Wang, Y. Wang, Y. Wang, Y. Wang, Z. Wang, Z. Wang, Z. Wang, G. Warnes, V. Warnsmann, H. Watada, E. Watanabe, M. Watchon, A. Wawrzynska, T. E. Weaver, G. Wegrzyn, A.M. Wehman, H. Wei, L. Wei, T. Wei, Y. Wei, O. H. Weiergraber, C.C. Weihl, G. Weindl, R. Weiskirchen, A. Wells, R.H. Wen, X. Wen, A. Werner, B. Weykopf, S.P. Wheatley, J.L. Whitton, A.J. Whitworth, K. Wiktorska, M.E. Wildenberg, T. Wileman, S. Wilkinson, D. Willbold, B. Williams, R.S.B. Williams, R.L. Williams, P.R. Williamson, R.A. Wilson, B. Winner, N. J. Winsor, S.S. Witkin, H. Wodrich, U. Woehlbier, T. Wollert, E. Wong, J.H. Wong, R.W. Wong, V.K.W. Wong, W.W. Wong, A.G. Wu, C. Wu, J. Wu, J. Wu, K.K. Wu, M. Wu, S.Y. Wu, S. Wu, S.Y. Wu, S. Wu, W.K.K. Wu, X. Wu, X. Wu, Y.W. Wu, Y. Wu, R.J. Xavier, H. Xia, L. Xia, Z. Xia, G. Xiang, J. Xiang, M. Xiang, W. Xiang, B. Xiao, G. Xiao, H. Xiao, H.T. Xiao, J. Xiao, L. Xiao, S. Xiao, Y. Xiao, B. Xie, C.M. Xie, M. Xie, Y. Xie, Z. Xie, Z. Xie, M. Xilouri, C. Xu, E. Xu, H. Xu, J. Xu, J. Xu, L. Xu, W. W. Xu, X. Xu, Y. Xue, S.M.S. Yakhine-Diop, M. Yamaguchi, O. Yamaguchi, A. Yamamoto, S. Yamashina, S. Yan, S.J. Yan, Z. Yan, Y. Yanagi, C. Yang, D. S. Yang, H. Yang, H.T. Yang, H. Yang, J.M. Yang, J. Yang, J. Yang, L. Yang, L. Yang, M. Yang, P.M. Yang, Q. Yang, S. Yang, S. Yang, S.F. Yang, W. Yang, W.Y. Yang, X. Yang, X. Yang, Y. Yang, Y. Yang, H. Yao, S. Yao, X. Yao, Y.G. Yao, Y.M. Yao, T. Yasui, M. Yazdankhah, P.M. Yen, C. Yi, X.M. Yin, Y. Yin, Z. Yin, Z. Yin, M. Ying, Z. Ying, C.K. Yip, S.P.T. Yiu, Y.H. Yoo, K. Yoshida, S.R. Yoshii, T. Yoshimori, B. Yousefi, B. Yu, H. Yu, J. Yu, J. Yu, L. Yu, M.L. Yu, S.W. Yu, V.C. Yu, W.H. Yu, Z. Yu, Z. Yu, J. Yuan, L.Q. Yuan, S. Yuan, S.F. Yuan, Y. Yuan, Z. Yuan, J. Yue, Z. Yue, J. Yun, R.L. Yung, D.N. Zacks, G. Zaffagnini, V.O. Zambelli, I. Zanella, Q. S. Zang, S. Zanivan, S. Zappavigna, P. Zaragoza, K.S. Zarbalis, A. Zarebkohan, A. Zarrouk, S.O. Zeitlin, J. Zeng, J.D. Zeng, E. Zerovnik, L. Zhan, B. Zhang, D. D. Zhang, H. Zhang, H. Zhang, H. Zhang, H. Zhang, H. Zhang, H. Zhang, H.L. Zhang, J. Zhang, J. Zhang, J.P. Zhang, K.Y.B. Zhang, L.W. Zhang, L. Zhang, L. Zhang, L. Zhang, L. Zhang, M. Zhang, P. Zhang, S. Zhang, W. Zhang, X. Zhang, X. W. Zhang, X. Zhang, X. Zhang, X. Zhang, X.D. Zhang, Y. Zhang, Y. Zhang, Y. Zhang, Y.D. Zhang, Y. Zhang, Y.Y. Zhang, Y. Zhang, Z. Zhang, Z. Zhang, Z. Zhang, Z. Zhang, Z. Zhang, H. Zhao, L. Zhao, S. Zhao, T. Zhao, X. F. Zhao, Y. Zhao, Y. Zhao, Y. Zhao, Y. Zhao, G. Zheng, K. Zheng, L. Zheng, S. Zheng, X.L. Zheng, Y. Zheng, Z.G. Zheng, B. Zhivotovsky, Q. Zhong, A. Zhou, B. Zhou, C. Zhou, G. Zhou, H. Zhou, H. Zhou, H. Zhou, J. Zhou, J. Zhou, J. Zhou, J. Zhou, K. Zhou, R. Zhou, X.J. Zhou, Y. Zhou, Y. Zhou, Y. Zhou, Z.Y. Zhou, Z. Zhou, B. Zhu, C. Zhu, G.Q. Zhu, H. Zhu, H. Zhu, H. Zhu, W.G. Zhu, Y. Zhu, Y. Zhu, H. Zhuang, X. Zhuang, K. Zientara-Rytter, C.M. Zimmermann, E. Ziviani, T. Zoladek, W. X. Zong, D.B. Zorov, A. Zorzano, W. Zou, Z. Zou, Z. Zou, S. Zuryn, W. Zwerschke, B. Brand-Saberi, X.C. Dong, C.S. Kenchappa, Z. Li, Y. Lin, S. Oshima, Y. Rong, J. C. Sluimer, C.L. Stallings, C.K. Tong, Guidelines for the use and interpretation of assays for monitoring autophagy, 4th edition)(1), Autophagy 17 (1) (2021) 1–382.

[42] Y. Sun, Y. Zheng, C. Wang, Y. Liu, Glutathione depletion induces ferroptosis, autophagy, and premature cell senescence in retinal pigment epithelial cells, Cell Death Dis. 9 (7) (2018) 753.

[43] H. Mancilla, R. Maldonado, K. Cereceda, F. Villarroel-Espindola, M. Montes de Oca, C. Angulo, M.A. Castro, J.C. Slebe, J.C. Vera, S. Lavandero, Concha, II, glutathione depletion induces spermatogonial cell autophagy, J. Cell. Biochem. 116 (10) (2015) 2283–2292.

[44] P. Szoka, J. Lachowicz, M. Cwiklinska, A. Lukaszewicz, A. Rybak, U. Baranowska, A. Holownia, Cigarette smoke-induced oxidative stress and autophagy in human alveolar epithelial cell line (A549 cells), Adv. Exp. Med. Biol. 1176 (2019) 63–69.

[45] J.R. Burgoyne, O. Oviosu, P. Eaton, The PEG-switch assay: a fast semi-quantitative method to determine protein reversible cysteine oxidation, J. Pharmacol. Toxicol. Methods 68 (3) (2013) 297–301.

[46] C. Mauvezin, T.P. Neufeld, Bafilomycin A1 disrupts autophagic flux by inhibiting both V-ATPase-dependent acidification and Ca-P60A/SERCA-dependent autophagosome-lysosome fusion, Autophagy 11(8) (2015) 1437–1438.

[47] W. Tian, R. Alsaadi, Z. Guo, A. Kalinina, M. Carrier, M.E. Tremblay, B. Lacoste, D. Lagace, R.C. Russell, An antibody for analysis of autophagy induction, Nat. Methods 17 (2) (2020) 232–239.

[48] J.F. Fahrmann, I. Tanaka, E. Irajizad, X. Mao, J.B. Dennison, E. Murage, J. Casabar, J. Mayo, Q. Peng, M. Celiktas, J.V. Vykoukal, S. Park, A. Taguchi, O. Delgado, S. C. Tripathi, H. Katayama, L.M.S. Soto, J. Rodriguez-Canales, C. Behrens, I. Wistuba, S. Hanash, E.J. Ostrin, Mutational activation of the NRF2 pathway upregulates kynureninase resulting in tumor immunosuppression and poor outcome in lung adenocarcinoma, Cancers 14 (10) (2022).

[49] L.D. Goldstein, J. Lee, F. Gnad, C. Klijn, A. Schaub, J. Reeder, A. Daemen, C. E. Bakalarski, T. Holcomb, D.S. Shames, R.J. Hartmaier, J. Chmielecki, S. Seshagiri, R. Gentleman, D. Stokoe, Recurrent loss of NFE2L2 exon 2 is a mechanism for Nrf2 pathway activation in human cancers, Cell Rep. 16 (10) (2016) 2605–2617.

[50] M. von Otter, P. Bergstrom, A. Quattrone, E.V. De Marco, G. Annesi, P. Soderkvist, S.B. Wettinger, M. Drozdzik, M. Bialecka, H. Nissbrandt, C. Klein, M. Nilsson, O. Hammarsten, S. Nilsson, H. Zetterberg, Genetic associations of Nrf2-encoding NFE2L2 variants with Parkinson's disease - a multicenter study, BMC Med. Genet. 15 (2014) 131.

[51] M. El Assar, J. Angulo, J.A. Carnicero, S. Walter, F.J. Garcia-Garcia, E. Lopez-Hernandez, J.M. Sanchez-Puelles, L. Rodriguez-Manas, Frailty is associated with lower expression of genes involved in cellular response to stress: results from the toledo study for healthy aging, J. Am. Med. Dir. Assoc. 18 (8) (2017), 734 e1-734 e7.

[52] Y. Xiang, L. Fu, H.X. Xiang, L. Zheng, Z.X. Tan, L.X. Wang, W. Cao, D.X. Xu, H. Zhao, Correlations among pulmonary DJ-1, vdr and nrf-2 in patients with chronic obstructive pulmonary disease: a case-control study, Int. J. Med. Sci. 18 (11) (2021) 2449–2456.

[53] A.M. Fratta Pasini, C. Stranieri, M. Ferrari, U. Garbin, L. Cazzoletti, C. Mozzini, F. Spelta, D. Peserico, L. Cominacini, Oxidative stress and Nrf2 expression in peripheral blood mononuclear cells derived from COPD patients: an observational longitudinal study, Respir. Res. 21 (1) (2020) 37.

[54] M. Suzuki, T. Betsuyaku, Y. Ito, K. Nagai, Y. Nasuhara, K. Kaga, S. Kondo, M. Nishimura, Down-regulated NF-E2-related factor 2 in pulmonary macrophages of aged smokers and patients with chronic obstructive pulmonary disease, Am. J. Respir. Cell Mol. Biol. 39 (6) (2008) 673–682.

[55] A. Dehnad, W. Fan, J.X. Jiang, S.R. Fish, Y. Li, S. Das, G. Mozes, K.A. Wong, K. A. Olson, G.W. Charville, M. Ali, N.J. Torok, AGER1 downregulation associates with fibrosis in nonalcoholic steatohepatitis and type 2 diabetes, J. Clin. Invest. 130 (8) (2020) 4320–4330.

[56] A. Anandhan, M. Dodson, A. Shakya, J. Chen, P. Liu, Y. Wei, H. Tan, Q. Wang, Z. Jiang, K. Yang, J.G. Garcia, S.K. Chambers, E. Chapman, A. Ooi, Y. Yang-Hartwich, B.R. Stockwell, D.D. Zhang, NRF2 controls iron homeostasis and ferroptosis through HERC2 and VAMP8, Sci. Adv. 9 (5) (2023) eade9585.

[57] P.J. Meakin, S. Chowdhry, R.S. Sharma, F.B. Ashford, S.V. Walsh, R.J. McCrimmon, A.T. Dinkova-Kostova, J.F. Dillon, J.D. Hayes, M.L. Ashford, Susceptibility of Nrf2-null mice to steatohepatitis and cirrhosis upon consumption of a high-fat diet is associated with oxidative stress, perturbation of the unfolded protein response, and disturbance in the expression of metabolic enzymes, but not with insulin resistance, Mol. Cell Biol. 34 (17) (2014) 3305–3320.

[58] R. Sabouny, E. Fraunberger, M. Geoffrion, A.C. Ng, S.D. Baird, R.A. Screaton, R. Milne, H.M. McBride, T.E. Shutt, The keap1-nrf2 stress response pathway promotes mitochondrial hyperfusion through degradation of the mitochondrial fission protein Drp1, Antioxidants Redox Signal 27 (18) (2017) 1447–1459.

[59] A.T. Dinkova-Kostova, A.Y. Abramov, The emerging role of Nrf2 in mitochondrial function, Free Radic. Biol. Med. 88 (2015) 179–188. Pt B.

[60] F. Bartolome, A.Y. Abramov, Measurement of mitochondrial NADH and FAD autofluorescence in live cells, Methods Mol. Biol. 1264 (2015) 263–270.

[61] L. Montava-Garriga, F. Singh, G. Ball, I.G. Ganley, Semi-automated quantitation of mitophagy in cells and tissues, Mech. Ageing Dev. 185 (2020) 111196.